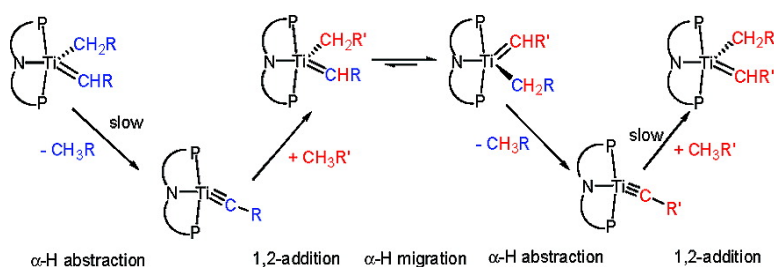


## Intermolecular C–H Bond Activation Reactions Promoted by Transient Titanium Alkylidynes. Synthesis, Reactivity, Kinetic, and Theoretical Studies of the Ti#C Linkage

Brad C. Bailey, Hongjun Fan, John C. Huffman, Mu-Hyun Baik, and Daniel J. Mindiola

*J. Am. Chem. Soc.*, **2007**, 129 (28), 8781-8793 • DOI: 10.1021/ja070989q • Publication Date (Web): 26 June 2007

Downloaded from <http://pubs.acs.org> on February 16, 2009



### More About This Article

Additional resources and features associated with this article are available within the HTML version:

- Supporting Information
- Links to the 16 articles that cite this article, as of the time of this article download
- Access to high resolution figures
- Links to articles and content related to this article
- Copyright permission to reproduce figures and/or text from this article

[View the Full Text HTML](#)



## Intermolecular C–H Bond Activation Reactions Promoted by Transient Titanium Alkylidynes. Synthesis, Reactivity, Kinetic, and Theoretical Studies of the Ti≡C Linkage

Brad C. Bailey, Hongjun Fan, John C. Huffman, Mu-Hyun Baik,\* and Daniel J. Mindiola\*

Contribution from the Molecular Structure Center and School of Informatics, Department of Chemistry, Indiana University, Bloomington, Indiana 47405

Received February 11, 2007; E-mail: mbaik@indiana.edu; mindiola@indiana.edu

**Abstract:** The neopentylidene–neopentyl complex (PNP)Ti=CH<sup>t</sup>Bu(CH<sub>2</sub><sup>t</sup>Bu) (**2**; PNP<sup>−</sup> = N[2-P(CHMe<sub>2</sub>)<sub>2</sub>-4-methylphenyl]<sub>2</sub>), prepared from the precursor (PNP)Ti=CH<sup>t</sup>Bu(OTf) (**1**) and LiCH<sub>2</sub><sup>t</sup>Bu, extrudes neopentane in neat benzene under mild conditions (25 °C) to generate the transient titanium alkylidyne, (PNP)Ti≡C<sup>t</sup>Bu (**A**), which subsequently undergoes 1,2-CH bond addition of benzene across the Ti≡C linkage to generate (PNP)Ti=CH<sup>t</sup>Bu(C<sub>6</sub>H<sub>5</sub>) (**3**). Kinetic, mechanistic, and theoretical studies suggest the C–H activation process to obey pseudo-first-order in titanium, the α-hydrogen abstraction to be the rate-determining step (KIE for 2/2-*d*<sub>5</sub> conversion to 3/3-*d*<sub>5</sub> = 3.9(5) at 40 °C) with activation parameters Δ*H*<sup>‡</sup> = 24(7) kcal/mol and Δ*S*<sup>‡</sup> = −2(3) cal/mol·K, and the post-rate-determining step to be C–H bond activation of benzene (primary KIE = 1.03(7) at 25 °C for the intermolecular C–H activation reaction in C<sub>6</sub>H<sub>6</sub> vs C<sub>6</sub>D<sub>6</sub>). A KIE of 1.33(3) at 25 °C arose when the intramolecular C–H activation reaction was monitored with 1,3,5-C<sub>6</sub>H<sub>3</sub>D<sub>3</sub>. For the activation of aromatic C–H bonds, however, the formation of the σ-complex becomes rate-determining via a hypothetical intermediate (PNP)Ti≡C<sup>t</sup>Bu(C<sub>6</sub>H<sub>5</sub>), and C–H bond rupture is promoted in a heterolytic fashion by applying standard Lewis acid/base chemistry. Thermolysis of **3** in C<sub>6</sub>D<sub>6</sub> at 95 °C over 48 h generates **3-*d*<sub>6</sub>**, thereby implying that **3** can slowly equilibrate with **A** under elevated temperatures with *k* = 1.2(2) × 10<sup>−5</sup> s<sup>−1</sup>, and with activation parameters Δ*H*<sup>‡</sup> = 31(16) kcal/mol and Δ*S*<sup>‡</sup> = 3(9) cal/mol·K. At 95 °C for one week, the EIE for the **2** → **3** reaction in 1,3,5-C<sub>6</sub>H<sub>3</sub>D<sub>3</sub> was found to be 1.36(7). When **1** is alkylated with LiCH<sub>2</sub>SiMe<sub>3</sub> and KCH<sub>2</sub>Ph, the complexes (PNP)Ti=CH<sup>t</sup>Bu(CH<sub>2</sub>SiMe<sub>3</sub>) (**4**) and (PNP)Ti=CH<sup>t</sup>Bu(CH<sub>2</sub>Ph) (**6**) are formed, respectively, along with their corresponding tautomers (PNP)Ti=CHSiMe<sub>3</sub>(CH<sub>2</sub><sup>t</sup>Bu) (**5**) and (PNP)Ti=CHPh(CH<sub>2</sub><sup>t</sup>Bu) (**7**). By means of similar alkylations of (PNP)Ti=CHSiMe<sub>3</sub>(OTf) (**8**), the degenerate complex (PNP)Ti=CHSiMe<sub>3</sub>(CH<sub>2</sub>SiMe<sub>3</sub>) (**9**) or the non-degenerate alkylidene–alkyl complex (PNP)Ti=CHPh(CH<sub>2</sub>SiMe<sub>3</sub>) (**11**) can also be obtained, the latter of which results from a tautomerization process. Compounds **4/5** and **9**, or **6/7** and **11**, also activate benzene to afford (PNP)Ti=CHR(C<sub>6</sub>H<sub>5</sub>) (R = SiMe<sub>3</sub> (**10**), Ph (**12**)). Substrates such as FC<sub>6</sub>H<sub>5</sub>, 1,2-F<sub>2</sub>C<sub>6</sub>H<sub>4</sub>, and 1,4-F<sub>2</sub>C<sub>6</sub>H<sub>4</sub> react at the aryl C–H bond with intermediate **A**, in some cases regioselectively, to form the neopentylidene–aryl derivatives (PNP)Ti=CH<sup>t</sup>Bu(aryl). Intermediate **A** can also perform stepwise alkylidene–alkyl metatheses with 1,3,5-Me<sub>3</sub>C<sub>6</sub>H<sub>3</sub>, SiMe<sub>4</sub>, 1,2-bis(trimethylsilyl)alkyne, and bis(trimethylsilyl)ether to afford the titanium alkylidene–alkyls (PNP)Ti=CHR(R') (R = 3,5-Me<sub>2</sub>C<sub>6</sub>H<sub>2</sub>, R' = CH<sub>2</sub>-3,5-Me<sub>2</sub>C<sub>6</sub>H<sub>2</sub>; R = SiMe<sub>3</sub>, R' = CH<sub>2</sub>SiMe<sub>3</sub>; R = SiMe<sub>2</sub>C≡CSiMe<sub>3</sub>, R' = CH<sub>2</sub>SiMe<sub>2</sub>C≡CSiMe<sub>3</sub>; R = SiMe<sub>2</sub>OSiMe<sub>3</sub>, R' = CH<sub>2</sub>SiMe<sub>2</sub>OSiMe<sub>3</sub>).

### 1. Introduction

The controlled and selective activation of inert C–H bonds of alkanes and arenes, and their functionalization to commodity products, is one of the major challenges that organotransition metal chemistry faces today, and constitutes an area of intense study.<sup>1–4</sup> Part of the challenge lies within the inert C–H bonds

that lack energetically accessible orbitals or binding sites to facilitate the activation process, unlike most substrates that are easier to activate, given their inherent binding affinity. This problem is often circumvented by preparing highly unsaturated metal complexes that are capable of interacting with the C–H bonds of the substrate. The most common routes to C–H activation involve either discrete oxidative addition<sup>5</sup> or σ-bond metathesis.<sup>6–9</sup> The former reaction typically implicates late transition metal complexes,<sup>7</sup> while the latter often applies

- (1) (a) Crabtree, R. H. *Chem. Rev.* **1985**, *85*, 245–69. (b) Bergman, R. G. *Science* **1984**, *223*, 902–8. (c) Graham, W. A. G. *J. Organomet. Chem.* **1986**, *300*, 81–91. (d) Halpern, J. *Inorg. Chim. Acta* **1985**, *100*, 41–8. (e) Crabtree, R. H.; Hamilton, D. G. *Adv. Organomet. Chem.* **1988**, *28*, 299–338. (f) Jones, W. D.; Feher, F. J. *Acc. Chem. Res.* **1989**, *22*, 91–100. (g) Shilov, A. E.; Shul'pin, G. B. *Chem. Rev.* **1997**, *97*, 2879–932. (h) Crabtree, R. H. *Dalton Trans.* **2001**, 2437–50.  
 (2) Duncan, A. P.; Bergman, R. G. *Chem. Rev.* **2002**, *2*, 431–45.  
 (3) Labinger, J. A.; Bercaw, J. E. *Nature* **2002**, *417*, 507–14.

- (4) Arndtsen, B. A.; Bergman, R. G.; Mobley, T. A.; Peterson, T. H. *Acc. Chem. Res.* **1995**, *28*, 154–62.

- (5) (a) Jones, W. D.; Hessel, E. T. *J. Am. Chem. Soc.* **1993**, *115*, 554–62. (b) Wang, C.; Ziller, J. W.; Flood, T. C. *J. Am. Chem. Soc.* **1995**, *117*, 1647–8.

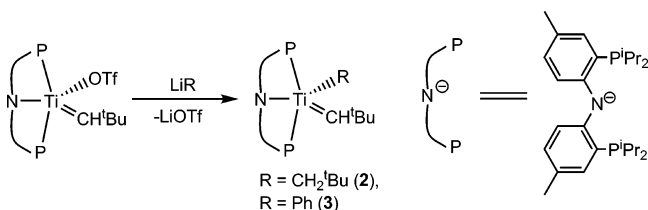
lanthanides, actinides, or early transition metals.<sup>6</sup> Radical bond homolysis,<sup>10</sup> electrophilic activation,<sup>11</sup> and 1,2-additions across a highly polarized metal–ligand multiple bond<sup>2,4,12–29</sup> encompass the remaining forms of C–H bond activation reactions known to date.

While a common goal of C–H activation chemistry is to functionalize the arene or alkane substrate to a synthetically useful product, finding a species that can initiate the C–H activation under controlled conditions can be regarded as one of the most difficult steps, especially if such a reaction can be performed selectively. Even though most existing transformations of alkane C–H bonds can be done by applying metal oxide

catalysts, such processes are often dominated by radical pathways encompassing H-atom removal, thus rendering the C–H activation step dependent on the C–H bond strength itself.<sup>3</sup> As a result, exploring C–H activation reactions with systems that avoid radical pathways would constitute an attractive paradigm, since selectivity would not be entirely dominated by the strength of the C–H bond. In a closed-shell formalism, transition metal alkylidenes and imides are an important class of ligands, given their implication not only in catalysis<sup>2,30</sup> but also in intermolecular alkane/arene C–H activation, in some cases regioselectively.<sup>2,21</sup> The latter type of transformation can be perhaps traced back to Bercaw and Rothwell,<sup>9,18,31</sup> who found that transient early transition metal alkylidenes could not only participate in metathesis-type chemistry but also engage in the intramolecular C–H activation of the ancillary ligand via 1,2-addition reactions across the M=CHR linkage (M = Ti, R = H; M = Ta, R = SiMe<sub>3</sub>).<sup>18,19</sup> To our knowledge, these results represent the first reported cases of an alkylidene endorsing a C–H activation step. Contrary to intramolecular 1,2-CH activation reactions,<sup>15,19,20,32–34</sup> intermolecular 1,2-addition of a C–H bond across a metal–ligand multiple bond is a far more scant but desired phenomenon, and such a transformation has been narrowly confined to M=NR<sup>2,13,15–17,22,24,27</sup> and M=CHR<sup>12,21,23,25,26,28</sup> functionalities. The first examples of such a process were reported by Wolczanski<sup>13</sup> and Bergman,<sup>22</sup> who demonstrated that unsaturated group 4 imides can trigger the activation of a variety of hydrocarbons, including methane in the case of Wolczanski's system. C–H activation across polarized metal–ligand multiple bonds was further expanded to the alkylidene series by Girolami,<sup>25</sup> Gibson,<sup>23</sup> Hessen,<sup>12</sup> and Legzdins.<sup>21,26,28</sup> In this respect, the latter type of systems are unique in the sense that they provide an opportunity to mechanistically study new and globally important reactions such as alkene and alkane metathesis.<sup>35</sup> From another applied perspective, C–H activation reactions involving metal–ligand multiply bonded functionalities such as the terminal oxo have also been studied employing bioinorganic mimics,<sup>36</sup> and have been implicated in monooxygenases.<sup>4,37</sup>

- (6) (a) Guram, A. S.; Jordan, R. F.; Taylor, D. F. *J. Am. Chem. Soc.* **1991**, *113*, 1833–5. (b) Thompson, M. E.; Baxter, S. M.; Bulls, A. R.; Burger, B. J.; Nolan, M. C.; Santarsiero, B. D.; Schaefer, W. P.; Bercaw, J. E. *J. Am. Chem. Soc.* **1987**, *109*, 203–19. (c) Watson, P. L.; Parshall, G. W. *Acc. Chem. Res.* **1985**, *18*, 51–6. (d) Fendrick, C. M.; Marks, T. J. *J. Am. Chem. Soc.* **1986**, *108*, 425–37.
- (7) Burger, P.; Bergman, R. G. *J. Am. Chem. Soc.* **1993**, *115*, 10462–3.
- (8) (a) Watson, P. L. *J. Am. Chem. Soc.* **1983**, *105*, 6491–3. (b) Vidal, V.; Theolier, A.; Thivolle-Cazat, J.; Basset, J.-M.; Coker, J. *J. Am. Chem. Soc.* **1996**, *118*, 4595–602. (c) Nicolai, G. P.; Basset, J.-M. *Appl. Catal. A* **1996**, *146*, 145–56.
- (9) Rothwell, I. P. *Acc. Chem. Res.* **1988**, *21*, 153–9.
- (10) (a) Sherry, A. E.; Wayland, B. B. *J. Am. Chem. Soc.* **1990**, *112*, 1259–61. (b) Wayland, B. B.; Ba, S.; Sherry, A. E. *J. Am. Chem. Soc.* **1991**, *113*, 5305–11.
- (11) Stahl, S.; Labinger, J. A.; Bercaw, J. E. *Angew. Chem., Int. Ed.* **1998**, *37*, 2181–92.
- (12) van der Heijden, H.; Hessen, B. *Chem. Commun.* **1995**, 145–6.
- (13) Cummins, C. C.; Baxter, S. M.; Wolczanski, P. T. *J. Am. Chem. Soc.* **1988**, *110*, 8731–3.
- (14) (a) Howard, W. A.; Waters, M.; Parkin, G. *J. Am. Chem. Soc.* **1993**, *115*, 4917–18. (b) Lee, S. Y.; Bergman, R. G. *J. Am. Chem. Soc.* **1995**, *117*, 5877–8. (c) Parkin, G.; Bercaw, J. E. *J. Am. Chem. Soc.* **1989**, *111*, 391–3. (d) Cook, G. K.; Mayer, J. M. *J. Am. Chem. Soc.* **1994**, *116*, 1855–68. (e) Legzdins, P.; Veltheer, J. E.; Young, M. A.; Batchelor, R. J.; Einstein, F. W. B. *Organometallics* **1995**, *14*, 407–17.
- (15) (a) Cummins, C. C.; Schaller, C. P.; Van Duyn, G. D.; Wolczanski, P. T.; Chan, A. W. E.; Hoffmann, R. *J. Am. Chem. Soc.* **1991**, *113*, 2985–94. (b) Schaller, C. P.; Wolczanski, P. T. *Inorg. Chem.* **1993**, *32*, 131–44. (c) de With, J.; Horton, A. D. *Angew. Chem., Int. Ed.* **1993**, *32*, 903–5. (d) Walsh, P. J.; Hollander, F. J.; Bergman, R. G. *Organometallics* **1993**, *12*, 3705–23. (e) Royo, P.; Sanchez-Nieves, J. *J. Organomet. Chem.* **2000**, *597*, 61–8. (f) Lee, S. Y.; Bergman, R. G. *J. Am. Chem. Soc.* **1995**, *117*, 5877–8. (g) Schaller, C. P.; Cummins, C. C.; Wolczanski, P. T. *J. Am. Chem. Soc.* **1996**, *118*, 591–611. (h) Polse, J. L.; Andersen, R. A.; Bergman, R. G. *J. Am. Chem. Soc.* **1998**, *120*, 13405–14. (i) Schafer, D. F., II; Wolczanski, P. T. *J. Am. Chem. Soc.* **1998**, *120*, 4881–2. (j) Hoyt, H. M.; Forrest, M. E.; Bergman, R. G. *J. Am. Chem. Soc.* **2004**, *126*, 1018–9.
- (16) Bennett, J. L.; Wolczanski, P. T. *J. Am. Chem. Soc.* **1994**, *116*, 2179–80.
- (17) (a) Schaller, C. P.; Bonanno, J. B.; Wolczanski, P. T. *J. Am. Chem. Soc.* **1994**, *116*, 4133–4. (b) Cundari, T. R.; Klinckman, T. R.; Wolczanski, P. T. *J. Am. Chem. Soc.* **2002**, *124*, 1481–7.
- (18) McDade, C.; Green, J. C.; Bercaw, J. E. *Organometallics* **1982**, *1*, 1629–34.
- (19) Chamberlain, L. R.; Rothwell, I. P.; Huffman, J. C. *J. Am. Chem. Soc.* **1986**, *108*, 1502–9.
- (20) Couturier, J. L.; Paillet, C.; Leconte, M.; Basset, J. M.; Weiss, K. *Angew. Chem.* **1992**, *31*, 628–31.
- (21) Pamplin, C. B.; Legzdins, P. *Acc. Chem. Res.* **2003**, *36*, 223–33.
- (22) Walsh, P. J.; Hollander, F. J.; Bergman, R. G. *J. Am. Chem. Soc.* **1988**, *110*, 8729–31.
- (23) Coles, M. P.; Gibson, V. C.; Clegg, W.; Elsegood, M. R. J.; Porrelli, P. A. *Chem. Commun.* **1996**, 1963–4.
- (24) Bennett, J. L.; Wolczanski, P. T. *J. Am. Chem. Soc.* **1997**, *119*, 10696–719.
- (25) Cheon, J.; Rogers, D. M.; Girolami, G. S. *J. Am. Chem. Soc.* **1997**, *119*, 6804–13.
- (26) (a) Tran, E.; Legzdins, P. *J. Am. Chem. Soc.* **1997**, *119*, 5071–2. (b) Adams, C. S.; Legzdins, P.; McNeil, W. S. *Organometallics* **2001**, *20*, 4939–55. (c) Adams, C. S.; Legzdins, P.; Tran, E. *Organometallics* **2002**, *21*, 1474–86. (d) Wada, K.; Pamplin, C. B.; Legzdins, P. *J. Am. Chem. Soc.* **2002**, *124*, 9680–1. (e) Wada, K.; Pamplin, C. B.; Legzdins, P.; Patrick, B. O.; Tsyba, I.; Bau, R. *J. Am. Chem. Soc.* **2003**, *125*, 7035–48. (f) Tsang, J. Y. K.; Buschhaus, M. S. A.; Legzdins, P.; Patrick, B. O. *Organometallics* **2006**, *25*, 4215–25.
- (27) Slaughter, L. M.; Wolczanski, P. T.; Klinckman, T. R.; Cundari, T. R. *J. Am. Chem. Soc.* **2000**, *122*, 7953–75.
- (28) Adams, C. S.; Legzdins, P.; Tran, E. *J. Am. Chem. Soc.* **2001**, *123*, 612–24.
- (29) Bailey, B. C.; Fan, H.; Baum, E. W.; Huffman, J. C.; Baik, M.-H.; Mindiola, D. J. *J. Am. Chem. Soc.* **2005**, *127*, 16016–7.
- (30) Schrock, R. R. *Chem. Rev.* **2002**, *102*, 145–79.
- (31) Chamberlain, L.; Rothwell, I. P.; Huffman, J. C. *J. Am. Chem. Soc.* **1982**, *104*, 7338–40.
- (32) (a) van Doorn, J. A.; van der Heijden, H.; Orpen, A. G. *Organometallics* **1994**, *13*, 4271–7. (b) van Doorn, J. A.; van der Heijden, H.; Orpen, A. G. *Organometallics* **1995**, *14*, 1278–83.
- (33) (a) Duncalf, D. J.; Harrison, R. J.; McCamley, A.; Royan, B. W. *Chem. Commun.* **1995**, 2421–2. (b) Minhas, R. K.; Scoles, L.; Wong, S.; Gambarotta, S. *Organometallics* **1996**, *15*, 1113–21. (c) Deckers, P. J. W.; Hessen, B. *Organometallics* **2002**, *21*, 5564–75. (d) Kickham, J. E.; Guerin, F.; Stephan, D. W. *J. Am. Chem. Soc.* **2002**, *124*, 11486–94. (e) Hanna, T. E.; Keresztes, I.; Lobkovsky, E.; Bernskoetter, W. H.; Chirik, P. J. *Organometallics* **2004**, *23*, 3448–58.
- (34) Basuli, F.; Bailey, B. C.; Huffman, J. C.; Mindiola, D. J. *Organometallics* **2005**, *24*, 3321–34.
- (35) (a) Goldman, A. S.; Roy, A. H.; Huang, Z.; Ahuja, R.; Schinski, W.; Brookhart, M. *Science* **2006**, *312*, 257–61. (b) Le Roux, E.; Taoufik, M.; Coperet, C.; de Mallmann, A.; Thivolle-Cazat, J.; Basset, J.-M.; Maunders, B. M.; Sunley, G. *J. Angew. Chem., Int. Ed.* **2005**, *44*, 6755–8. (c) Soulvong, D.; Coperet, C.; Thivolle-Cazat, J.; Basset, J.-M.; Maunders, B. M.; Pardy, R. B. A.; Sunley, G. *J. Angew. Chem., Int. Ed.* **2004**, *43*, 5366–9. (d) Coperet, C.; Maury, O.; Thivolle-Cazat, J.; Basset, J.-M. *Angew. Chem., Int. Ed.* **2001**, *40*, 2331–4. (e) Basset, J. M.; Coperet, C.; Lefort, L.; Maunders, B. M.; Maury, O.; Le Roux, E.; Saggio, G.; Soignier, S.; Soulvong, D.; Sunley, G. J.; Taoufik, M.; Thivolle-Cazat, J. *J. Am. Chem. Soc.* **2005**, *127*, 8604–5. (f) Basset, J.-M.; Coperet, C.; Soulvong, D.; Taoufik, M.; Thivolle-Cazat, J. *Angew. Chem., Int. Ed.* **2006**, *45*, 6082–5. (g) Blanc, F.; Coperet, C.; Thivolle-Cazat, J.; Basset, J.-M. *Angew. Chem., Int. Ed.* **2006**, *45*, 6201–3. (h) Blanc, F.; Coperet, C.; Thivolle-Cazat, J.; Basset, J.-M.; Lesage, A.; Emsley, L.; Sinha, A.; Schrock, R. R. *Angew. Chem., Int. Ed.* **2006**, *45*, 1216–20.

Scheme 1

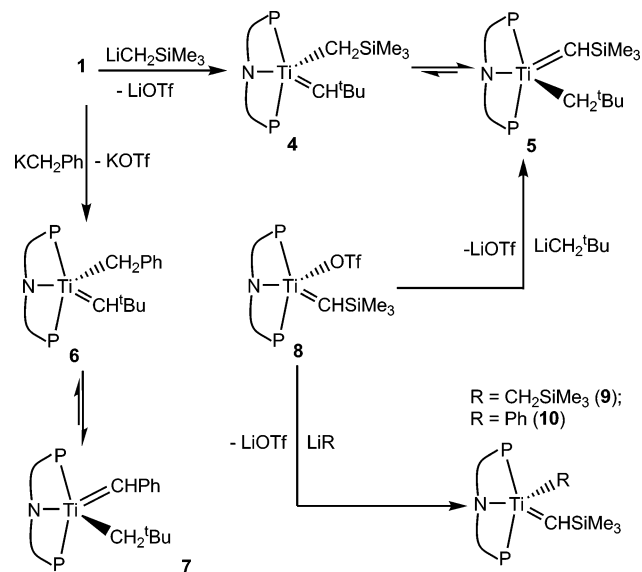


Given the remarkable reactivity observed with alkylidenes, we postulated that generation of an early transition metal alkylidyne may afford an even more potent and polarized M–C multiple bond, which could enable us to perform unique transformations under non-forcing conditions. We have recently shown that transient  $\text{Ti}\equiv\text{C}$  linkages<sup>29</sup> can, in fact, be generated in situ, and can now be added to the short list of metal–ligand multiply bonded systems that activate the C–H bonds of hydrocarbons under mild conditions. In this work, we thoroughly investigate the steps leading to and involved in the C–H activation of benzene by applying a combination of experimental kinetic studies and molecular reaction modeling based on density functional theory. In addition, we report regioselective aryl C–H activation reactions with a variety of substrates and propose that the binding event of the substrate can direct the C–H activation process. The product formation in these reactions appears to be under kinetic more than thermodynamic control. Among our attempts at regioselective C–H activation, we also discovered that the  $\text{Ti}\equiv\text{C}$  linkage can engage in alkylidene–alkyl metathesis via multiple C–H activation reactions of tetramethylsilane and hydrocarbons by employing a combination of 1,2-CH addition,  $\alpha$ -hydrogen migration, and  $\alpha$ -hydrogen abstraction steps.

## 2. Results and Discussion

**2.1. Synthesis and Characterization of Titanium Alkylidene–Alkyl Complexes.**  $\text{LiCH}_2^t\text{Bu}$  reacts cleanly with  $(\text{PNP})\text{Ti}=\text{CH}^t\text{Bu}(\text{OTf})$  (**1**;  $\text{PNP}^- = \text{N}[2\text{-P}(\text{CHMe}_2)_2\text{-4-methylphenyl}]_2$ )<sup>39</sup> to afford the neopentylidene–neopentyl complex  $(\text{PNP})\text{Ti}=\text{CH}^t\text{Bu}(\text{CH}_2^t\text{Bu})$  (**2**) in 88% yield (Scheme 1). The transmetalation step must be performed quickly in pentane (or  $\text{C}_6\text{H}_{12}$ ) to avoid rapid decomposition of **2** (vide infra). Solids of **2**, however, are relatively stable when stored at  $-35\text{ }^\circ\text{C}$  ( $t_{1/2} \approx 2$  months). Evidence for  $\alpha$ -hydrogen migration between the neopentylidene and neopentyl fragments in **2** was supported by reaction of **1** with  $\text{LiCD}_2^t\text{Bu}$  to rapidly provide **2-d<sub>2</sub>**, which exists as a 1:2 mixture of isotopomers  $(\text{PNP})\text{Ti}=\text{CH}^t\text{Bu}(\text{CD}_2^t\text{Bu})$  and  $(\text{PNP})\text{Ti}=\text{CD}^t\text{Bu}(\text{CDH}^t\text{Bu})$ , respectively, as judged by  $^1\text{H}$  or  $^{31}\text{P}$  NMR spectra (see Supporting Information). Thus,  $\alpha$ -hy-

Scheme 2

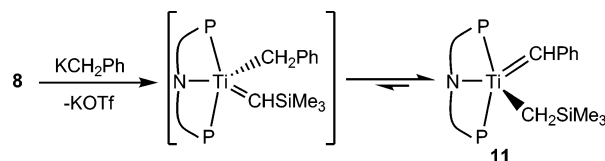


drogen migration in **2** is rapid on the chemical time scale (minutes) in solution phase but slow on the NMR time scale. Other alkyl groups can be readily incorporated with retention of the neopentylidene unit. For example, 1 equiv of  $\text{LiPh}$  reacts cleanly with **1** in  $\text{Et}_2\text{O}$  to afford the alkylidene–phenyl derivative  $(\text{PNP})\text{Ti}=\text{CH}^t\text{Bu}(\text{C}_6\text{H}_5)$  (**3**) (Scheme 1). Tautomers also arise when the alkyl group deviates from neopentyl and contains  $\alpha$ -hydrogens. Consequently, when **1** was treated with 1 equiv of  $\text{LiCH}_2\text{SiMe}_3$  or  $\text{KCH}_2\text{Ph}$ ,<sup>40</sup> a mixture of the alkylidenes  $(\text{PNP})\text{Ti}=\text{CH}^t\text{Bu}(\text{CH}_2\text{SiMe}_3)$  (**4**)<sup>29</sup>/ $(\text{PNP})\text{Ti}=\text{CHSiMe}_3(\text{CH}_2^t\text{Bu})$  (**5**)<sup>29</sup> or  $(\text{PNP})\text{Ti}=\text{CH}^t\text{Bu}(\text{CH}_2\text{Ph})$  (**6**)/ $(\text{PNP})\text{Ti}=\text{CHPh}(\text{CH}_2^t\text{Bu})$  (**7**) was observed at  $25\text{ }^\circ\text{C}$  via a combination of  $^1\text{H}$ ,  $^{13}\text{C}$ , and  $^{31}\text{P}$  NMR spectra (Scheme 2). Mixtures of **4/5** or **6/7** are formed by  $\alpha$ -hydrogen migration from the alkyl ligand to the neopentylidene  $\alpha$ -carbon.<sup>30</sup> Stronger evidence for the tautomerization of **4/5** or **6/7** can be collected by an independent synthetic route forming the species in question. This conjecture is shown to be correct since transmetalation of  $(\text{PNP})\text{Ti}=\text{CHSiMe}_3(\text{OTf})$  (**8**) with  $\text{LiCH}_2^t\text{Bu}$  generates identical ratios of **4/5**, thereby suggesting a  $4 \leftrightarrow 5$  equilibrium scenario (Scheme 2). While  $\alpha$ -hydrogen migration among complexes bearing alkyl, alkylidene, and alkylidyne substituents has been documented,<sup>30,41–45</sup>  $\alpha$ -hydrogen migration amid non-degenerate alkyl, alkylidene, and alkylidyne ligands is an exceedingly rare phenomenon, given the low number of known archetypical systems.<sup>30,34,46</sup> In the case of degenerate systems, similar tautomerization processes involving Ta,<sup>44</sup> W,<sup>42</sup> and Os<sup>45</sup> have been documented by Schrock and Xue, and this phenomenon appears to occur at much slower chemical time scales than in our systems. The

(36) (a) Costas, M.; Chen, K.; Que, L. *Coord. Chem. Rev.* **2000**, *200*, 200–202, 517–44. (b) Hirao, H.; Kumar, D.; Que, L., Jr.; Shaik, S. *J. Am. Chem. Soc.* **2006**, *128*, 8590–606. (c) Kaizer, J.; Klinker, E. J.; Oh, N. Y.; Rohde, J.-U.; Song, W. J.; Stubna, A.; Kim, J.; Muenck, E.; Nam, W.; Que, L., Jr. *J. Am. Chem. Soc.* **2004**, *126*, 472–3. (37) (a) Que, L., Jr.; Dong, Y. *Acc. Chem. Res.* **1996**, *29*, 190–6. (b) Rosenzweig, A. C.; Lippard, S. *J. Am. Chem. Res.* **1994**, *27*, 229–36. (c) Baik, M.-H.; Newcomb, M.; Friesner, R. A.; Lippard, S. *J. Chem. Rev.* **2003**, *103*, 2385–419. (d) Du Bois, J.; Mizoguchi, T. J.; Lippard, S. *J. Coord. Chem. Rev.* **2000**, *200*–202, 443–85. (38) Bailey, B. C.; Huffman, J. C.; Mindaola, D. J.; Weng, W.; Ozerov, O. V. *Organometallics* **2005**, *24*, 1390–3. (39) (a) Fan, L.; Foxman, B. M.; Ozerov, O. V. *Organometallics* **2004**, *23*, 326–8. (b) Fan, L.; Yang, L.; Guo, C.; Foxman, B. M.; Ozerov, O. V. *Organometallics* **2004**, *23*, 4778–87. (c) Ozerov, O. V.; Guo, C.; Fan, L.; Foxman, B. M. *Organometallics* **2004**, *23*, 5573–80. (d) Ozerov, O. V.; Guo, C.; Papkov, V. A.; Foxman, B. M. *J. Am. Chem. Soc.* **2004**, *126*, 4792–3.

(40) Schlosser, M.; Hartmann, J. *Angew. Chem.* **1973**, *85*, 544–5. (41) Liu, X.; Li, L.; Diminnie, J. B.; Yap, G. P. A.; Rheingold, A. L.; Xue, Z. *Organometallics* **1998**, *17*, 4597–606. (42) Chen, T.; Wu, Z.; Li, L.; Sorasane, K. R.; Diminnie, J. B.; Pan, H.; Guzei, I. A.; Rheingold, A. L.; Xue, Z. *J. Am. Chem. Soc.* **1998**, *120*, 13519–20. (43) (a) Morton, L. A.; Zhang, X.-H.; Wang, R.; Lin, Z.; Wu, Y.-D.; Xue, Z.-L. *J. Am. Chem. Soc.* **2004**, *126*, 10208–9. (b) Morton, L. A.; Wang, R.; Yu, X.; Campana, C. F.; Guzei, I. A.; Yap, G. P. A.; Xue, Z.-L. *Organometallics* **2006**, *25*, 427–34. (44) Schrock, R. R.; Fellmann, J. D. *J. Am. Chem. Soc.* **1978**, *100*, 3359–70. (45) LaPointe, A. M.; Schrock, R. R.; Davis, W. M. *J. Am. Chem. Soc.* **1995**, *117*, 4802–13. (46) (a) Caulton, K. G.; Chisholm, M. H.; Streib, W. E.; Xue, Z. *J. Am. Chem. Soc.* **1991**, *113*, 6082–90. (b) Xue, Z.; Chuang, S.-H.; Caulton, K. G.; Chisholm, M. H. *Chem. Mater.* **1998**, *10*, 2365–70. (c) Xue, Z.; Caulton, K. G.; Chisholm, M. H. *Chem. Mater.* **1991**, *3*, 384–6.

Scheme 3

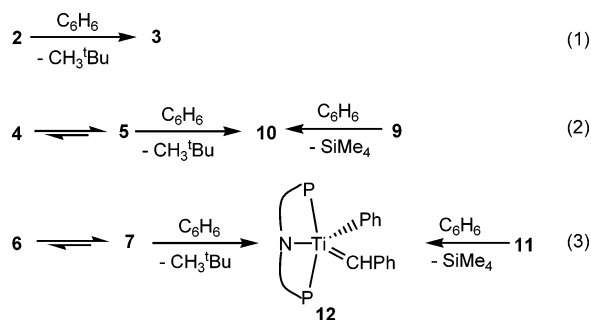


difference in the rate of tautomerization might be a consequence of the meridional constraint imposed by the PNP framework, resulting in the alkylidene and alkyl groups being more proximal to one another, thus rendering the H atom more susceptible to 1,3-migration.

Analogous to the degenerate  $\alpha$ -hydrogen migration reaction in **2**, treatment of **8** with  $\text{LiCH}_2\text{SiMe}_3$  yields the complex  $(\text{PNP})\text{Ti}=\text{CHSiMe}_3(\text{CH}_2\text{SiMe}_3)$  (**9**) (Scheme 2). The triflate group in **8** can also be replaced with  $\text{Ph}^-$  to afford a close relative of **3**, namely  $(\text{PNP})\text{Ti}=\text{CHSiMe}_3(\text{C}_6\text{H}_5)$  (**10**) (Scheme 2).<sup>29</sup> Treatment of **8** with  $\text{KCH}_2\text{Ph}$  results in essentially complete tautomerization to the benzylidene derivative,  $(\text{PNP})\text{Ti}=\text{CHPh}(\text{CH}_2\text{SiMe}_3)$  (**11**), via the intermediate  $(\text{PNP})\text{Ti}=\text{CHSiMe}_3(\text{CH}_2\text{Ph})$  (inferred from NMR spectra, Scheme 3). All alkylidene–alkyl systems reported here are far less vulnerable to intramolecular ancillary ligand degradation when compared to other titanium derivatives previously prepared in our laboratory using the sterically encumbering  $\beta$ -diketiminate ligand.<sup>34</sup>

Alkylidene–alkyl compounds **2–7** and **9–11** display  $^{13}\text{C}$  NMR resonances between 253 and 310 ppm, indicative of each system bearing a terminal alkylidene functionality. These complexes also reveal relatively low  $J_{\text{C-H}}$  coupling constants of 86–99 Hz for the alkylidene carbon, in addition to a low-field  $\alpha$ -H resonance (6.76–13.00 ppm).<sup>30</sup> The latter two parameters suggest strongly that an agostic  $\alpha$ -hydrogen interaction with the electron-deficient metal center is present.<sup>30</sup> The  $C_2$ -symmetric nature of the pincer framework renders complexes **2–7** and **9–11** chiral, which is clearly manifested by each system having two sets of doublets in its  $^{31}\text{P}$  NMR spectrum. Furthermore, the inequivalent phosphines display low  $J_{\text{P-P}}$  coupling constants of 32–53 Hz, an indication that the PNP framework is significantly skewed from a rigid trans geometry.

**2.2. C–H Activation of Benzene. 2.2.1.  $\alpha$ -Hydrogen Abstraction Reactions and C–H Activation.** Compounds **2**, **4–7**, **9**, and **11** are all kinetic products under  $\text{N}_2$  inasmuch as they activate the C–H bond of benzene (eqs 1–3). While the neopentylidene–neopentyl complex **2** reacts with  $\text{C}_6\text{H}_6$  at 27 °C over  $\sim 12$  h to afford the phenyl derivative **3** and  $\text{CH}_3^t\text{Bu}$  (eq 1), the **4/5** mixture also transforms smoothly (15 h at 30 °C) in  $\text{C}_6\text{H}_6$  to form *only one alkylidene product*, namely compound **10** (eq 2). Likewise, the **6/7** mixture of alkylidenes gradually decay in  $\text{C}_6\text{H}_6$  at 30 °C over 48 h to also produce one compound, the benzylidene–phenyl derivative  $(\text{PNP})\text{Ti}=\text{CHPh}(\text{Ph})$  (**12**) (eq 3). Complex **12** can also be generated, albeit slowly, from C–H activation of benzene via the thermolysis of **11** ( $\sim 80\%$  conversion at 60 °C over 3 days), but unfortunately other products are formed in the reaction mixture. Complex **11** clearly shows that the benzylidene complex is the preferred tautomer compared to the corresponding (trimethylsilyl)methylidene. Hence, the reactivity of the alkylidene unit decreases in the sequence  $\text{Ti}=\text{CH}^t\text{Bu} \gg \text{Ti}=\text{CHSiMe}_3 \geq \text{Ti}=\text{CHPh}$ . This trend is further corroborated by



the rate of reactions involving  $\text{C}_6\text{H}_6$  and the alkylidene–alkyl precursor or mixture. Whereas complex **2** transforms to **3** with  $t_{1/2} = 3.1$  h, tautomeric mixtures **4/5** and **6/7** react much slower with benzene. Complex **9**, on the other hand, appears to transform in  $\text{C}_6\text{H}_6$  to **10** at a rate that is comparably slower relative to that for the **4/5** mixture. Likewise, **11** also transforms very slowly, which may give rise to undesirable competing side reactions. In accord with these observations, we infer that the stability of the trimethylmethylidene motif arises from dissipation of electron density away from the alkylidene  $\alpha$ -C via strengthening of the C–Si bond by  $\sigma$ -hyperconjugation, which decreases the nucleophilicity of the  $\alpha$ -C. In the case of the  $\text{Ti}=\text{CHPh}$  functionality, the negative charge at the  $\alpha$ -C is likely minimized by delocalization onto the phenyl group (vide infra). Steric effects may also play a role in the stability of each system, since complex **2** has the most crowded environment. As it will be described below, elimination of alkane is one of the key steps along the transformation of complexes such as **2**.

**2.2.2. Structural Characterization of Titanium Alkylidene–Alkyl Complexes.** In order to establish the degree of  $\alpha$ -H agostic interaction in the alkylidene–alkyl complexes, we collected single-crystal X-ray diffraction data for compounds **2**, **3**, **11**, and **12** (Figure 1). Crystal structure data for **2** and **3** have been reported in an earlier communication.<sup>29</sup> Although the molecular structure of **2** lies with the Ti and N atoms on the 2-fold axis at  $1/4, y, 3/4$ , where the  $\text{Ti}=\text{CH}^t\text{Bu}$  and  $\text{Ti}-\text{CH}_2^t\text{Bu}$  groups are disordered about this axis, these motifs are well resolved, with none of the atomic positions overlapping. The partial occupancy hydrogen atoms associated with the disordered ligands were clearly visible in a difference Fourier map, and a slightly better model was obtained when the methyl hydrogen atoms were placed in idealized riding positions. Similar structural disorders have been recently observed with tungsten bis(alkylidene)/alkylidyne–alkyl tautomers.<sup>41</sup> In all cases, the molecular structures reveal short Ti=C bonds (1.790(5) Å, **2**; 1.873(5) Å, **3**; 1.876(2) Å, **11**; 1.889(2) Å, **12**)<sup>12,29,30,32,34,38,47,48</sup> and indicate a metal center residing in a pseudo-trigonal-bipyramidal geometry, where the two phosphine groups occupy

- (47) (a) Krueger, C.; Mynott, R.; Siedenbiedel, C.; Stehling, L.; Wilke, G. *Angew. Chem.* **1991**, *103*, 1714–15. (b) Kahlert, S.; Gorls, H.; Scholz, J. *Angew. Chem., Int. Ed.* **1998**, *37*, 1857–61. (c) Van de Heisteg, B. J. J.; Schat, G.; Akkerman, O. S.; Bickelhaupt, F. *J. Organomet. Chem.* **1986**, *310*, C25–8. (d) Baumann, R.; Stumpf, R.; Davis, W. M.; Liang, L.-C.; Schrock, R. R. *J. Am. Chem. Soc.* **1999**, *121*, 7822–36. (e) Hartner, F. W., Jr.; Schwartz, J.; Clift, S. M. *J. Am. Chem. Soc.* **1983**, *105*, 640–1. (f) Scholz, J.; Goerls, H. *Organometallics* **2004**, *23*, 320–2. (g) Sinnema, P.-J.; van der Veen, L.; Spek, A. L.; Veldman, N.; Teuben, J. H. *Organometallics* **1997**, *16*, 4245–7. (h) Bailey, B. C.; Basuli, F.; Huffman, J. C.; Mendiola, D. J. *Organometallics* **2006**, *25*, 3963–8. (i) Mendiola, D. J. *Acc. Chem. Res.* **2006**, *39*, 813–21. (j) Mendiola, D. J.; Bailey, B. C.; Basuli, F. *Eur. J. Inorg. Chem.* **2006**, 3335–46.
- (48) (a) Basuli, F.; Bailey, B. C.; Tomaszewski, J.; Huffman, J. C.; Mendiola, D. J. *J. Am. Chem. Soc.* **2003**, *125*, 6052–3. (b) Basuli, F.; Bailey, B. C.; Watson, L. A.; Tomaszewski, J.; Huffman, J. C.; Mendiola, D. J. *Organometallics* **2005**, *24*, 1886–906.

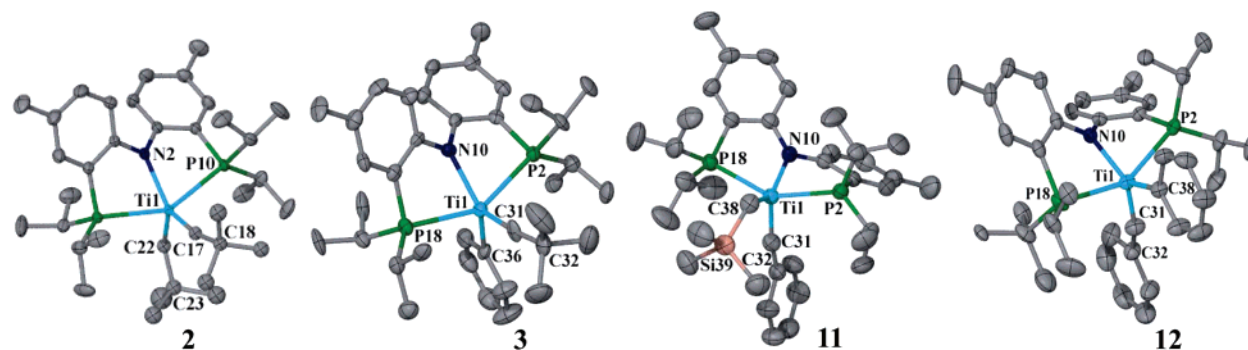


**Figure 1.** Molecular structures of complexes **2**, **3**, **11**, and **12**, depicting thermal ellipsoids at the 50% probability level. Solvent and H-atoms have been excluded for clarity. Selected metrical parameters (distances in angstroms, angles in degrees): For **2**, Ti1–N2, 2.124(3); Ti1–P10, 2.6003(6); Ti1–C17, 1.790(5); Ti1–C22, 2.206(5); Ti1–C17–C18, 166.3(4); Ti1–C22–C23, 133.4(4); P10A–Ti1–P10, 148.59(3). For **3**, Ti1–N10, 2.089(4); Ti1–P2, 2.580(8); Ti1–P18, 2.612(8); Ti1–C31, 1.873(5); Ti1–C36, 2.141(5); Ti1–C31–C32, 174.7(5); P2–Ti1–P18, 149.70(6). For **11**: Ti1–N10, 2.061(6); Ti1–P2, 2.561(1); Ti1–P18, 2.607(1); Ti1–C31, 1.876(2); Ti–C38, 2.166(2); Ti1–C31–C32, 164.0(8); Ti1–C38–Si39, 126.2(3); P2–Ti1–P18, 147.75(3). For **12**: Ti1–N10, 2.029(5); Ti1–P2, 2.5360(6); Ti1–P18, 2.5840(6); Ti1–C31, 1.889(2); Ti1–C38, 2.146(8); Ti1–C31–C32, 159.2(7); P2–Ti1–P18, 150.70(2).

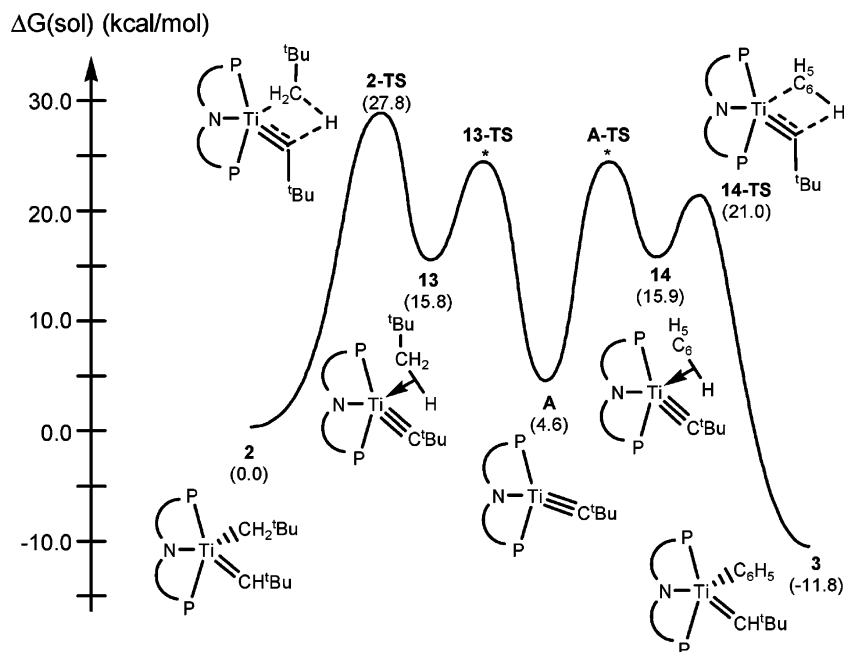


**Figure 2.** Computed reaction energy profile for **2** → **3** conversion in benzene ( $\epsilon = 2.284$ ). Relative energies in kcal/mol are given in parentheses. The transition states marked with asterisks cannot be located with standard methods and are estimated; see text for details.

the axial positions. As expected, the obtuse Ti=C–C angles (Figure 1) coupled with the low  $\alpha$ -C  $J_{C-H}$  (vide supra) are consistent with  $\alpha$ -H agostic interactions being present in both solution and solid phases. The molecular structure of **12** is unique, as it constitutes a rare example of a terminal titanium benzylidene complex.<sup>30</sup> Strong evidence for tautomerization in some of our systems originates from the molecular structure of **11** (Figure 1), exposing a rare example of a non-degenerate alkylidene–alkyl system bearing  $\alpha$ -hydrogens at both the alkylidene and alkyl functionalities.<sup>34,46</sup> While Ti–CH<sub>2</sub>SiMe<sub>3</sub> formation is evident from the acute Ti–C–Si angle (126.2(3)°) and Ti–C distance (2.166(2) Å), the Ti=C distance (vide supra) and distorted Ti=C–C angle (164.0(8)°) for the benzylidene unit in **11** are also consistent with  $\alpha$ -hydrogen migration from the formal benzyl to the former trimethylsilylmethylidene motif (Figure 1).

**2.2.3. Theoretical Studies.** To better understand the C–H activation mechanism, we turned to density functional theory (DFT) calculations and simulated the reaction of **2** → **3**

considering a number of reasonable mechanistic scenarios. Figure 2 summarizes the most plausible reaction pathway, and the computed structures of the key intermediates and transition states are shown in Figure 3. Complex **2** first undergoes  $\alpha$ -hydrogen abstraction, traversing the transition state **2-TS** at 27.8 kcal/mol to afford the hypothetical  $\sigma$ -complex (PNP)Ti≡CtBu(CH<sub>3</sub>tBu) (**13**), which is 15.8 kcal/mol higher in solution-phase free energy than **2**. Rapid entropy-assisted loss of neopentane yields the reactive titanium alkylidyne intermediate **A**, which is only slightly higher in energy than **2**, with a relative free energy of 4.6 kcal/mol. Locating the transition state for loss of neopentane (**13-TS**) is, unfortunately, impossible with standard quantum mechanical methods, because entropy plays an important and non-trivial role in determining this transition-state energy. Our simplistic approach only probes the electronic surface, however, and projects onto the free energy space by adding the entropy after the minima and first-order saddle points are located. We assume, therefore, that the electronic and free energy surfaces are sufficiently similar.

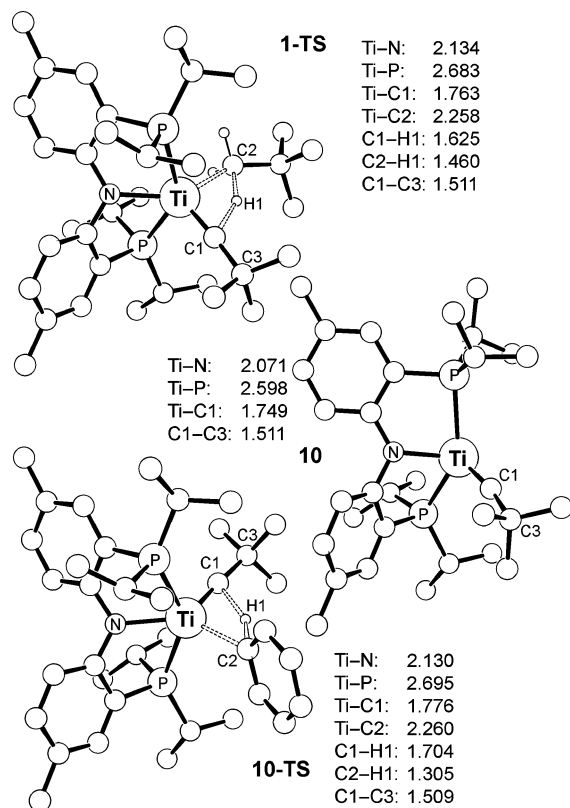


**Figure 3.** Computed structures of **2-TS**, **A**, and **14-TS**. Bond lengths are given in angstroms.

Whereas this assumption is plausible, it is not expected to be valid for ligand dissociation transition states that are dominated by entropy changes. Intuitively, we do not expect this transition state to be competitive with **2-TS**, as it is unlikely that the simple dissociation of neopentane to afford **A** is kinetically less facile than the C–H activation step to re-form **2**, which our calculations suggest to be associated with a barrier of 12.0 kcal/mol.

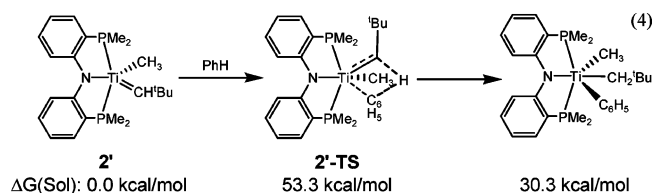
Upon addition of benzene, the titanium alkylidyne intermediate **A** first forms a  $\sigma$ -complex (PNP)Ti $\equiv$ C<sup>t</sup>Bu(C<sub>6</sub>H<sub>6</sub>) (**14**), which undergoes 1,2-addition of the C–H bond of the arene across the reactive Ti $\equiv$ C linkage to produce the final product **3**. Although we are unable to locate the transition state **A-TS**, which connects complex **A** with the  $\sigma$ -complex **14**, as we explained for **13-TS** (vide supra), we have some experimental evidence for **A-TS** being slightly higher in energy than **14-TS**, which must be traversed to form the final phenyl–alkylidene product **3**. This asymmetry of the reaction energy profile is interesting and highlights the significant difference between the activation of aliphatic and aromatic C–H bonds, with the computed  $\Delta\Delta G^\ddagger$  being 6.8 kcal/mol, which translates to several orders of magnitude difference in the rate.<sup>16,24</sup> When the titanium alkylidyne complex **A** reacts with an alkane, such as neopentane, the C–H activation process is rate-determining. For the activation of aromatic C–H bonds, however, the formation of the  $\sigma$ -complex becomes rate-determining. This difference is illustrated in Figure 2 by the computed energy differences between the  $\sigma$ -complexes and their respective C–H activation transition states. The energy difference between **13** and **2-TS** is 12.0 kcal/mol, whereas the energy difference between **14** and **14-TS** is only 5.1 kcal/mol. Thus, our calculations suggest that aliphatic C–H bonds are significantly more difficult to activate

than aromatic C–H bonds using the titanium alkylidyne complex.<sup>24</sup> The activation energy for cleaving the aromatic C–H bond is, in fact, so low that the formation of the aromatic  $\sigma$ -complex becomes rate-determining. This result is not intuitive, since aromatic C–H bonds are typically stronger than aliphatic C–H bonds by  $\sim 10$ – $15$  kcal/mol.<sup>49</sup> However, this observation is not unprecedented, since the kinetic preference for the stronger sp<sup>2</sup> C–H bond activation versus the sp<sup>3</sup> C–H bond vis-à-vis  $\Delta G^\ddagger_{\text{addition}}(\text{R}^2\text{H}) - \Delta G^\ddagger_{\text{addition}}(\text{R}^1\text{H})$  values<sup>16,24</sup> has been extensively investigated and discussed by Wolczanski, and such selectivity has been ascribed to the relative free energies of three-coordinate titanium imide precursors by applying a more compressed reaction coordinate.<sup>24</sup> Legzdins has also observed similar selectivities for sp<sup>2</sup> C–H bond activation reactions.<sup>28</sup>  $\pi$ -Orbital involvement of the sp<sup>2</sup> C–H substrate has been repeatedly suggested as an explanation to why there is more stabilization at the TS. By attaining shorter bond lengths with the sp<sup>2</sup>-hybridized substituent, H-transfer occurs over a much shorter distance and with minimal reorganization energy, hence resulting in an earlier TS for **14** versus late for **2** (vide infra). Consequently, the 1,2-CH bond addition step for the latter type will be prompted over sp<sup>3</sup> C–H substrate activation.<sup>16,24</sup> As mentioned above, our computed reaction energy profile places the titanium alkylidyne intermediate **A** at a relative energy of 4.6 kcal/mol compared to **2**, suggesting that **A** may be accessible at room temperature under equilibrium conditions and in the absence of reactive substrates. Experimental efforts toward exploiting this theoretical insight and detecting **A** directly are currently underway.

There are, of course, a few plausible mechanistic alternatives that deserve attention. For example, given the precedence for unsaturated M=C linkages to undergo intramolecular 1,2-CH addition of arenes,<sup>12,21,23,25,26,28</sup> we inquired whether or not complex **2** could engage in C–H activation events prior to the  $\alpha$ -hydrogen abstraction event (eq 4). Similar processes have been documented for imide analogues.<sup>2,13,15–17,22,24,27</sup> Using a slightly simplified model (PNP')Ti=CH<sup>t</sup>Bu(CH<sub>3</sub>) (**2'**; PNP'<sup>−</sup> = N[2-P(CH<sub>3</sub>)<sub>2</sub>phenyl]<sub>2</sub>) instead of **2**, we explored this alternative mechanistic scenario and found this reaction path to be both thermodynamically and kinetically unreasonable. Our calculations show that the putative six-coordinate intermediate (PNP')-Ti(CH<sub>2</sub><sup>t</sup>Bu)(CH<sub>3</sub>)(C<sub>6</sub>H<sub>5</sub>) is 30.3 kcal/mol higher in solution-phase free energy than the titanium alkylidene complex **2'**, indicating that the alkylidene moiety is thermodynamically unable to perform the C–H activation (even in a less congested environment provided by our simplified models). In addition, the lowest energy transition state was found at 53.3 kcal/mol, further supporting our conclusion that this reaction path is not accessible. There are a few other possible reaction channels to consider; e.g., the long Ti–P bond ( $>2.5$  Å) could break to release some of the steric crowding and electronic strain that we found for the putative mechanism outlined in eq 4. Despite much effort, we were unable to locate another reaction mechanism that was competitive to our proposed pathway involving the in situ formation of the titanium alkylidyne intermediate **A**. The most notable mechanistic alternatives that we considered are highlighted in the Supporting Information.

A more detailed examination of the computed transition-state structures of **2-TS** and **14-TS** (Figure 3) revealed structural

(49) Jones, W. D.; Feher, F. J. *J. Am. Chem. Soc.* **1982**, *104*, 4240–2.



elements that are intuitively expected for a  $\sigma$ -bond metathesis invoking transient metallacycles. In **2-TS**, the C1–H1–C2 arrangement is not linear per se ( $151.7^\circ$ ), and the C1–H1 bond is nearly broken at a bond length of  $1.625 \text{ \AA}$ , whereas the C2–H1 for the leaving neopentane is nearly formed at a distance of  $1.460 \text{ \AA}$ . Thus, the transition state **2-TS** can be considered “late” with respect to the titanium alkylidyne formation. In the case of **14-TS**, the C1–H1–C2 arrangement is similar to that in **2-TS** ( $152.7^\circ$ ), but the C1–H1 is even longer, at  $1.704 \text{ \AA}$ , when compared to the C2–H1 linkage ( $1.305 \text{ \AA}$ ). This feature strongly implies that the computed transition-state structure of **14-TS** can be regarded as “early” with respect to formation of **3**. On the basis of these observations, the C–H–C array in **2-TS** and **14-TS** can also be referred to as a three-center, four-electron ( $3c-4e$ ) system undergoing a proton transfer promoted by the Ti(IV) center.<sup>50</sup> For both **2-TS** and **14-TS**, there is small perturbation of the Ti≡C linkage ( $1.763$  and  $1.776 \text{ \AA}$ , respectively) and metrical parameters concerning the (PNP)Ti surrogate (see Supporting Information). Titanium alkylidyne character is fully developed at the transition state, with a Ti–C1 distance of  $1.763 \text{ \AA}$ . The Ti–C distance becomes  $1.749 \text{ \AA}$  in intermediate **A**, which we assign to a Ti≡C triple bond. As expected, the Ti≡C bond is significantly shorter than Ti=C and Ti–C moieties that were found for systems such as **2**, **3**, and **11**. For example, Ti=C and Ti–C distances in **2** were computed to be  $1.847$  and  $2.137 \text{ \AA}$ , respectively. Although it is reasonable to interpret the unusually short Ti–C distance obtained in our computer model of **A** as a strong indicator of a triple bond, a few different interpretations are equally plausible. Most interesting among these alternatives for the bonding in the Ti≡C fragment is formally invoking intramolecular ligand-to-metal charge transfer to afford a Ti(III)=C $\cdot$  moiety, which may adopt an open-shell singlet state, where the two unpaired electrons on Ti and C reside in spatially different orbitals but with opposite spins. These non-classical electronic structure patterns have recently received much attention,<sup>51</sup> and there is growing awareness that intramolecular M–L redox events may play a pivotal role in catalysis.<sup>52</sup> The question of whether a Ti(IV)=C or a Ti(III)=C $\cdot$  fragment is responsible for the remarkable reactivity of an intermediate such as **A** is crucial for designing more optimized reagents, because it has immediate consequences for the underlying driving force in the C–H activation mechanism. Despite significant efforts, including the use of manually constructed Kohn–Sham functions that were consistent with the open-shell singlet state as initial guesses,<sup>53</sup> we were unable to obtain a properly converged electronic structure that is expected for a Ti(III)=C $\cdot$  fragment. Instead, our calculations

(50) Werkema, E. L.; Maron, L.; Eisenstein, O.; Andersen, R. A. *J. Am. Chem. Soc.* **2007**, *129*, 2529–41.

(51) Ray, K.; Bill, E.; Weyhermuller, T.; Wieghardt, K. *J. Am. Chem. Soc.* **2005**, *127*, 5641–54.

(52) (a) Bart, S. C.; Chlopek, K.; Bill, E.; Bouwkamp, M. W.; Lobkovsky, E.; Neese, F.; Wieghardt, K.; Chirik, P. J. *J. Am. Chem. Soc.* **2006**, *128*, 13901–12. (b) Scott, J.; Gambarotta, S.; Korobkov, I.; Budzelaar, P. H. M. *J. Am. Chem. Soc.* **2005**, *127*, 13019–29.

(53) Yang, X.; Baik, M.-H. *J. Am. Chem. Soc.* **2006**, *128*, 7476–85.

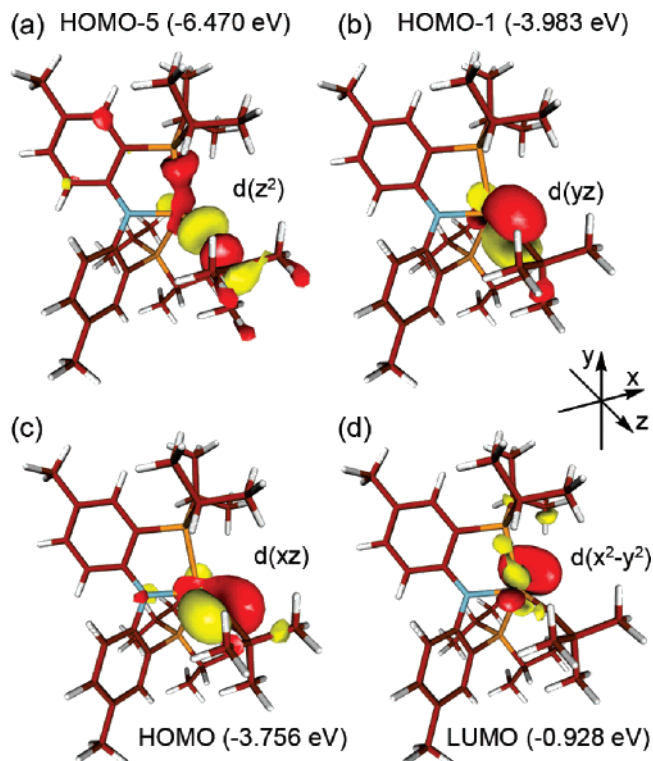


**Figure 4.** Most important molecular orbitals of **A** (isodensity = 0.05 au).

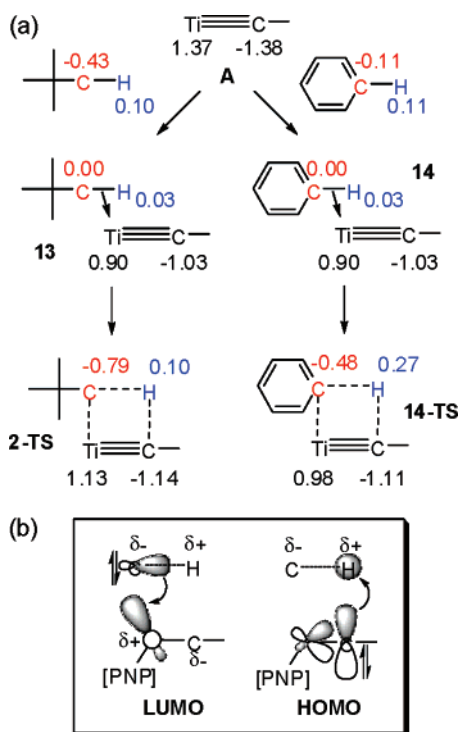
strongly support the presence of a Ti(IV)=C fragment in **A** with a Mayer bond order of 2.49, which is the projected value for a Ti–C triple bond.<sup>54</sup> For comparison, bond orders of 1.74 and 0.85 were computed in **2** for the Ti=C and Ti–C bonds, respectively.

Figure 4 shows the most important molecular orbitals of intermediate **A**. The HOMO–5, HOMO–1, and HOMO are easily recognized as the  $\sigma$ -orbital and the two orthogonal  $\pi$ -orbitals establishing the Ti≡C bond, respectively (Figure 4a–c). The LUMO (Figure 4d) is a M–L nonbonding orbital, mainly consisting of the metal  $d(x^2-y^2)$  orbital and significantly extending into the empty coordination site to facilitate binding of substrate. As this MO can be considered to be purely metal-based and fully decoupled from the ligand orbitals, we expect that utilization of the MO for binding additional ligands will have very little effect on both the geometry and the electronic structure of the titanium complex. Clearly, this is one of the key features that the structurally rigid (PNP)Ti framework provides. Being able to bind substrate to afford the  $\sigma$ -complex in this case, and doing so without causing significant electronic disruptions, is an important characteristic for the unparalleled reactivity of such a system.

Once the  $\sigma$ -complex (**13** and **14** in Figure 2) is formed between the reactant and the alkylidyne intermediate **A**, there are two possible formal mechanisms by which the C–H bond activation can take place. First, the C–H bond could be broken in a homolytic fashion at the transition state, which must be matched by a similarly homolytic cleavage of the triple bond of the titanium alkylidyne moiety to formally afford a Ti(III)=C $\cdot$  fragment. In this case, the  $\sigma$ -bond metathesis reaction is driven by the radical recombination energy. Alternatively, the C–H bond can also be envisioned to break heterolytically,

(54) Baik, M.-H.; Friesner, R. A.; Parkin, G. *Polyhedron* **2004**, *23*, 2879–900.





**Figure 5.** (a) ESP-fit charges of the titanium alkylidyne, the  $\sigma$ -complex, and the transition states. (b) Conceptualized MO interaction patterns leading to the heterolytic cleavage of the C–H bond.

matched by the corresponding heterolytic cleavage of the Ti–C triple bond. In this case, the C–H activation reaction is promoted by standard Lewis acid/base binding; viz., the titanium center serves as a strong Lewis acid, and the C–H bond of benzene attacks in a nucleophilic fashion. The electronic structure described in Figure 4 favors the latter scenario in principle, and our calculated transition states show highly charge-polarized transition states. Figure 5 summarizes the charge distribution at the titanium alkylidyne motif during the reaction with neopentane and benzene, monitored using charges that are fit to the electrostatic potentials (ESPs).<sup>55</sup> Our calculations assign charges of +1.37 to the titanium and –1.38 to the alkydine carbon in **A**. These ESP-fit charges must not be interpreted as an indication that a “carbanion” has been formed and/or the Ti≡C linkage is ionic, as the absolute values of quantum mechanically computed charges are not physically meaningful per se. The ESP charges merely indicate that the alkydine carbon is relatively electron-rich, resulting from the three main M–L bond MOs (Figure 4) being essentially dominated by carbon-based atomic orbitals. In addition, the <sup>t</sup>Bu group supplies extra electron density to lower-lying MOs, making the carbon even more electron-rich. More meaningful are the differential charges during the reaction. They serve as reporters of the electronic reorganizations that promote the reaction. Most importantly, our calculations indicate that the transition states **2-TS** and **14-TS** are both highly polarized (Figure 5). The carbon of the C–H bond that undergoes activation becomes negatively polarized at the transition states, with computed differential charges of –0.26 and –0.48 for **2-TS** and **14-TS**, respectively, compared to the  $\sigma$ -complexes **13** and **14** (Figure 5).

Figure 5b illustrates the electronic changes that are most consistent with our MO and charge analyses. At the transition state, the C–H bond breaks in a formally heterolytic fashion to

afford a negatively polarized C, whereas the H becomes positively polarized. The titanium alkylidyne moiety is already highly polarized and undergoes only a slight charge adjustment to match the induced dipole of the C–H of the substrate. The C–H carbon acts as a Lewis base and begins to form the C–Ti bond by interacting with the metal-based LUMO via the adduct **13** or **14**. At the same time, the Lewis-acidic C–H proton begins to interact with the alkydine carbon to formally complete the cleavage of one of the Ti–C triple bonds. The  $\sigma$ -bond metathesis is therefore driven by a closed-shell mechanism whereby the HOMO and LUMO of the metal-complex fragment interact in a cooperative fashion to activate and then break the C–H bond of the alkane or arene. Our calculations do not support a radical-recombination-type mechanism, which would be expected to show much less polarized transition states.

This analysis implies that electron-donating substituents on the alkydine moiety are important for its reactivity. Electron-withdrawing groups will diminish the charge polarization of the titanium alkylidyne carbon and therefore reduce the overall reactivity toward  $\sigma$ -bond metathesis. This conclusion is in good agreement with the experimental observation that the titanium alkylidyne precursors **4/5**, **6/7**, **9**, and **11** are less reactive toward C–H activation of benzene than the neopentylidyne precursor **2**. Based on these arguments, our theoretical analysis predicts that negative charge polarization at the alkydine carbon should follow the decaying order Ti≡C<sup>t</sup>Bu >> Ti≡CSiMe<sub>3</sub> ≥ Ti≡CPh, which would also explain their trend in reactivity.

#### 2.2.4. Kinetic Studies of the C–H Activation of Benzene.

Complex **2** was reacted with C<sub>6</sub>D<sub>6</sub> to confirm that (PNP)Ti=CD<sup>t</sup>Bu(C<sub>6</sub>D<sub>5</sub>) (**3-d**<sub>6</sub>) was quantitatively formed. Both <sup>1</sup>H and <sup>2</sup>H NMR spectra of **3-d**<sub>6</sub> reveal >99+% <sup>2</sup>H incorporation into the  $\alpha$ -carbon without <sup>2</sup>H scrambling into the PNP ligand framework. In C<sub>6</sub>D<sub>6</sub>, conversion of **2** → **3-d**<sub>6</sub> generates only CH<sub>3</sub><sup>t</sup>Bu, supporting our hypothesis that  $\alpha$ -abstraction in **2** should precede the C–H activation of benzene and that the overall slow step of the reaction is formation of a high-energy intermediate species. The fact that the PNP ancillary ligand was not involved in the C–H activation pathway narrowed our list of mechanistic possibilities.

#### 2.2.5. Kinetic Studies of the Rate-Determining Step.

Kinetic parameters for the conversion of **2** → **3** were assessed experimentally by monitoring the decay of **2** using <sup>31</sup>P NMR spectroscopy in C<sub>6</sub>D<sub>6</sub> to reveal a  $k_{\text{average}} = 6.5(4) \times 10^{-5} \text{ s}^{-1}$  at 27 °C. The reaction was found to obey pseudo-first-order kinetics in titanium, which is in good agreement with the reaction energy profile suggested by our DFT calculations (Figure 2). Unfortunately, under a depleted amount of benzene (e.g., C<sub>6</sub>D<sub>12</sub> as a medium), formation of **2** is not clean, given the promiscuity of intermediate **A** to react rapidly with both benzene and other media, such as cyclohexane, hexane, and pentane (vide infra). Temperature dependence studies of the **2** → **3** conversion between 15 and 40 °C allowed for extraction of the activation parameters  $\Delta H^\ddagger = 24(7) \text{ kcal/mol}$  and  $\Delta S^\ddagger = -2(3) \text{ cal/mol}\cdot\text{K}$  from the Eyring plot, thereby yielding a  $\Delta G^\ddagger$  value of  $\sim 24.7 \text{ kcal/mol}$  at 298.15 K (Figure 6), which is in reasonable agreement with the DFT prediction of 27.8 kcal/mol. The intermolecular  $k_{\text{H}}/k_{\text{D}}$  ratio is remarkably close to unity (1.03(3) at 25 °C) when the C–H activation reaction is carried out in C<sub>6</sub>H<sub>6</sub> vs C<sub>6</sub>D<sub>6</sub>, and remains essentially the same in a 1:1

(55) Breneman, C. M.; Wiberg, K. B. *J. Comput. Chem.* **1990**, *11*, 361–73.

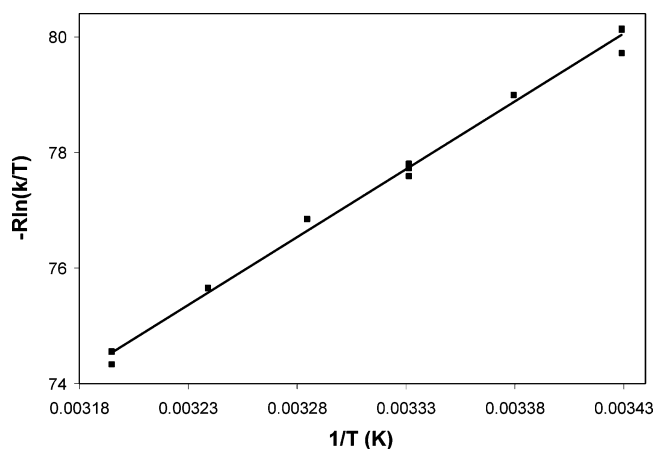


**Figure 6.** Eyring plot for the  $2 \rightarrow 3\text{-}d_6$  transformation in  $C_6D_6$ .

mixture of  $C_6H_6$  and  $C_6D_6$  (1.03(7) at 25 °C). In fact, only the latter competitive intermolecular KIE experiment in  $C_6D_6$  and  $C_6H_6$  will provide information about the substrate binding event, but, given the value close to unity, we conclude that the overall rate of the reaction has minor contributions from the C–H bond cleavage of benzene.<sup>56</sup> However, the rates are substantially different when the decays of **2** and **2-*d*<sub>3</sub>**, (PNP)Ti=CD<sup>t</sup>Bu-(CD<sub>2</sub><sup>t</sup>Bu), in benzene are measured, yielding a  $k_H/k_D$  ratio of 3.9(5) at 40 °C (at 27 °C, the  $k_H/k_D$  ratio was 3.7). Although this primary KIE deviates from unity, the value is not as large as the KIEs reported by Wolczanski (KIE = ~5–14).<sup>16,24</sup> This difference in KIE might be rationalized on the basis of a more asymmetric transfer of  $H^+$  from the  $C_{alkylidene}$  to the  $C_{alkyl}$  group proposed in our four-centered TS of **2**. As described earlier, our computed transition-state structure for **2-TS** reveals a C–H–C angle of 151.7° (vide supra), which could account for the lower KIE. In summary, these data provide strong evidence for the rate-determining step being the  $\alpha$ -abstraction to generate a transient titanium alkylidyne linkage. The 1,2-CH bond addition of benzene across the Ti≡C<sup>t</sup>Bu functionality is most likely not rate-determining. Since the highest barrier in the C–H bond activation process is  $\alpha$ -hydrogen abstraction, one would expect only a small contribution from secondary isotope effects and/or equilibrium isotope effects.<sup>56,57</sup> As it will turn out, the latter process does not contribute significantly to the KIE values obtained at 25 or 40 °C (vide infra).

### 2.2.6. Kinetic Studies of the Post-Rate-Determining Step.

Our DFT calculations suggest that both the C–H and C–D activation steps should be reversible, since the backward reaction for the C–H activation,  $3 \rightarrow A$  or  $3 \rightarrow 14$ , is associated with a barrier  $\geq 33$  kcal/mol. Therefore, conversion of **3**  $\rightarrow$  **A** should be overcome at a slow but reasonable rate under elevated temperature conditions (Figure 2). Gratifyingly, we determined that **3-*d*<sub>6</sub>** can slowly regenerate the alkylidyne **A** in  $C_6H_6$  at 100 °C within 48 h to afford **3**, while the latter (after purification) converts in neat  $C_6D_6$  back to **3-*d*<sub>6</sub>**, thus linking the alkylidyne intermediate **A** to the final product.<sup>9</sup> Kinetic parameters for the conversion of **3** to **3-*d*<sub>6</sub>** were assessed by monitoring the decay of **3** using <sup>1</sup>H NMR spectroscopy in  $C_6D_6$ , to reveal a  $k_{average} = 1.2(2) \times 10^{-5} s^{-1}$  at 95 °C. Albeit using a narrow temperature range, our temperature-dependent studies

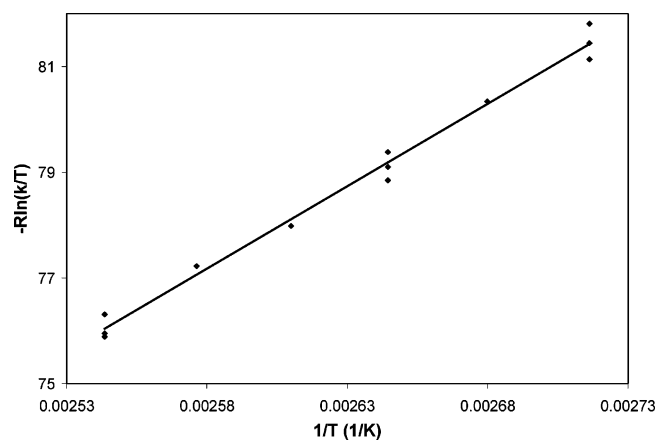


**Figure 7.** Eyring plot for the  $3 \rightarrow 3\text{-}d_6$  transformation in  $C_6D_6$ .

of the  $3 \rightarrow 3\text{-}d_6$  conversion between 95 and 120 °C allowed for extraction of the activation parameters<sup>9</sup>  $\Delta H^\ddagger = 31(16)$  kcal/mol and  $\Delta S^\ddagger = 3(9)$  cal/mol·K, which yielded a  $\Delta G^\ddagger$  value of ~30.1 kcal/mol at 298.15 K (Figure 7). The latter parameter is in excellent agreement with the DFT prediction of at least 32.8 kcal/mol for the reverse reaction,  $3 \rightarrow 14$  (Figure 2). For the  $2 \rightarrow 3$  and  $3 \rightarrow 3\text{-}d_6$  conversions, the errors affiliated with the activation parameters were determined by error propagation methods that include uncertainties for both rates and temperature, and which were derived from the Eyring equation (see Supporting Information).<sup>58</sup>

As suggested by Wolczanski and co-workers, 1,2-CH bond addition across the M=N functionality could involve a short-lived  $\sigma$ -bonded alkane intermediate.<sup>17</sup> To examine the C–H activation pathway stemming from **2** in greater detail and to determine whether or not an intermediate is formed, we resorted to the isotopically enriched benzene-1,3,5-*d*<sub>3</sub> reagent, previously used by Jones and co-workers to separate isotope effects that originate from intramolecular C–H activation processes from the intermolecular effects that are present when a 1:1 mixture of  $C_6H_6/C_6D_6$  is used.<sup>56,59</sup> Having only two chemically identical, isotopically marked reaction sites in this substrate provides a means of discerning whether or not secondary isotope effects play a significant role in the post-rate-determining step. In addition, the intramolecular kinetic isotope effect should give details about other intermediates that may be present along the activation and breaking of the C–H bond.

When **2** was treated with benzene-1,3,5-*d*<sub>3</sub>, <sup>1</sup>H NMR spectral analysis revealed a  $k_H/k_D$  ratio of 1.33(3), quantified by integrating the aromatic regions of the NMR spectra. Since **3** does not exchange with  $C_6D_6$  to **3-*d*<sub>6</sub>** under these conditions (25 °C), these results indicate that this  $k_H/k_D$  ratio reflects mostly contributions from both the substrate binding event (post-rate-determining) and the C–H bond activation step. This value does not originate from an equilibrium isotope effect (EIE), given the high barrier for the  $3 \rightarrow A$  conversion under these conditions.<sup>27</sup> Independent measurements of the EIE ( $2 \rightarrow 3$  conversion in benzene-1,3,5-*d*<sub>3</sub> at 95 °C for one week) do, in fact, reveal this value to be minor but comparable to the intramolecular KIE (1.36(7), see Supporting Information). Our KIE and EIE values therefore suggest that contributions from

(56) Jones, W. D. *Acc. Chem. Res.* **2003**, *36*, 140–6.

(57) Carpenter, B. K. *Determination of Organic Reaction Mechanisms*; Wiley-Interscience: New York 1984.

(58) Morse, P. M.; Spencer, M. D.; Wilson, S. R.; Girolami, G. S. *Organometallics* **1994**, *13*, 1646–55.

(59) Jones, W. D.; Feher, F. J. *J. Am. Chem. Soc.* **1986**, *108*, 4814–19.

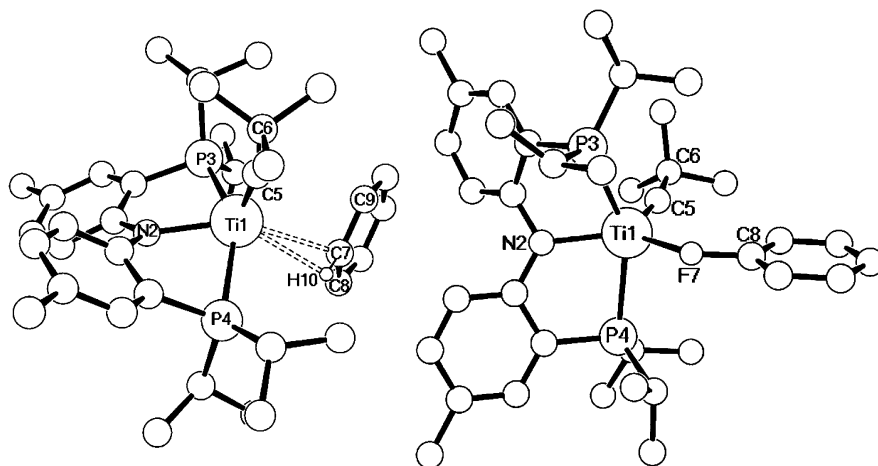


**Figure 8.** Computed structure for the proposed intermediates **14** (left) and  $(\text{PNP})\text{Ti}=\text{C}^t\text{Bu}(\text{FC}_6\text{H}_5)$  (right), depicting selected bond lengths (angstroms) and angles (degrees): For **14**, Ti1–C7, 2.739; Ti1–H10, 2.412; Ti1–N2, 2.097; Ti1–C5, 1.751; H10–C7, 1.092; 1.751; Ti1–C5–C6, 169.2; P3–Ti1–P4, 147.9. For  $(\text{PNP})\text{Ti}=\text{C}^t\text{Bu}(\text{FC}_6\text{H}_5)$ , Ti1–F7, 2.269; F7–C8, 1.398; Ti1–N2, 2.094; Ti1–C5, 1.753; Ti1–C5–C6, 165.9; Ti1–F7–C8, 136.2; P3–Ti1–P4, 147.7.

the C–H bond activation step are likely operative. Although the magnitude is small between the inter- and intramolecular KIEs ( $\Delta = 0.33$ ), and could be the net result of more complicated secondary isotopes effects, we propose that this discrepancy in the intra- vs intermolecular KIE originates from the substrate binding event being rate-determining as well as from contributions from C–H and C–D activations; i.e., **A-TS** must be higher in energy than **14-TS**, as illustrated in Figure 2. This result also implies that the  $\Delta\Delta G^\ddagger$  between **A-TS** and **14-TS** should be small, albeit detectable via the intramolecular KIE experiment. As a result, our data suggest that the barrier from **14** to **A** should be small and in the range of  $\sim 5.1$  kcal/mol (Figure 2, vide supra). Alternatively, our intramolecular KIE value could also reflect a fast equilibrium between C–H and C–D bound  $\sigma$ -complexes of benzene-1,3,5- $d_3$  from a  $\pi$ -complex prior to the C–H/C–D bond activation process. Intermediate **14**, which we identify as a  $\sigma$ -adduct, could of course be in equilibrium with a corresponding  $\pi$ -complex,  $(\text{PNP})\text{Ti}=\text{C}^t\text{Bu}(\eta^x\text{-C}_6\text{H}_6)$  ( $x = 2, 4, 6$ ), and we have no method to discard these possible intermediates during formation of the  $\sigma$ -complex prior to the C–H bond-breaking event.<sup>56,59</sup> In fact, given the ability of  $d^0$  metal complexes to readily form  $\pi$ -complexes in general,<sup>34,48,60</sup> the existence of a  $\pi$ -complex is plausible to propose. Despite substantial efforts, we were unable to find any stable adduct consistent with a  $\pi$ -complex in our computer models. All attempts at enforcing a  $\text{Ti}-\eta^{2-6}(\text{C}_6\text{H}_6)$  binding mode converged to the  $\sigma$ -adduct **14** in our geometry optimizations. Apparently, the titanium center in the Ti alkylidene complex is too hard (or too sterically crowded) to accommodate the soft  $\pi$ -base and prefers the relatively hard  $\sigma$ -base instead.

Since we did not detect any intermolecular KIE (1.03(3)–1.07(3)), we also propose that our intramolecular KIE can be interpreted to implicate an intermediate **14** that does not have significant rehybridization at the  $\text{sp}^2$  carbon.<sup>57</sup> Unfortunately, our noncompetitive KIE experiment does not provide conclusive evidence for the binding event being rate-determining after formation of **A**, since the  $\alpha$ -hydrogen abstraction from **2** is the overall rate-determining step. Taken together, our experimental and theoretical work suggests that the  $\sigma$ -complex **14** is a likely intermediate that connects the titanium alkylidene and the C–H

activation transition state (Figure 8). A  $\pi$ -complex, if formed, may rapidly rearrange or equilibrate to the  $\sigma$ -complex. As expected, the computed structure for the  $\sigma$ -complex of **14** reveals an essentially intact  $(\text{PNP})\text{Ti}=\text{C}^t\text{Bu}$  fragment with a weak interaction with the C–H bond of benzene. The metrical parameters reflect subtle changes from that of free benzene, as enumerated in Figure 8.

**2.3. Intermolecular C–H Activation Reactions of Substituted Arenes.** In addition to benzene, complex **2** reacts cleanly with other  $\text{sp}^2$  C–H bonds in substituted arenes. When treated with neat solvent, complex **2** generates **A**, which subsequently reacts with the arene C–H bond of the solvent to form the corresponding titanium alkylidene complex, having a substituted aryl group ligand. Accordingly, when complex **2** is dissolved in solvents such as fluorobenzene, 1,2-difluorobenzene, and 1,4-difluorobenzene, the alkylidene derivatives  $(\text{PNP})\text{-Ti}=\text{CH}^t\text{Bu}(\text{Ar}')$  ( $\text{Ar}' = o\text{-FC}_6\text{H}_4$  (**15**),  $o\text{-1,2-F}_2\text{C}_6\text{H}_2$  (**16**),  $1,4\text{-F}_2\text{C}_6\text{H}_3$  (**17**)) are quantitatively generated when assayed via  $^1\text{H}$ ,  $^{13}\text{C}$ , and  $^{31}\text{P}$  NMR spectroscopy (Figure 9). Unfortunately, toluene and *m*-xylene afforded at least three products when judged by  $^{31}\text{P}\{^1\text{H}\}$  NMR spectroscopy. When 1,3-difluorobenzene was used, two compounds were evident by  $^{31}\text{P}\{^1\text{H}\}$  NMR spectra (see Supporting Information), thus suggesting that aryl C–H activation is not regioselective for the former and latter

- (60) (a) Carpentier, J.-F.; Wu, Z.; Lee, C. W.; Stroemberg, S.; Christopher, J. N.; Jordan, R. F. *J. Am. Chem. Soc.* **2000**, *122*, 7750–67. (b) Casey, C. P.; Carpenetti, D. W., II; Sakurai, H. *J. Am. Chem. Soc.* **1999**, *121*, 9483–4. (c) Casey, C. P.; Hallenbeck, S. L.; Pollock, D. W.; Landis, C. R. *J. Am. Chem. Soc.* **1995**, *117*, 9770–1. (d) Casey, C. P.; Hallenbeck, S. L.; Wright, J. M.; Landis, C. R. *J. Am. Chem. Soc.* **1997**, *119*, 9680–90. (e) Casey, C. P.; Klein, J. F.; Fagan, M. A. *J. Am. Chem. Soc.* **2000**, *122*, 4320–30. (f) Casey, C. P.; Lee, T.-Y.; Tunge, J. A.; Carpenetti, D. W., II. *J. Am. Chem. Soc.* **2001**, *123*, 10762–3. (g) Casey, C. P.; Tunge, J. A.; Lee, T.-Y.; Fagan, M. A. *J. Am. Chem. Soc.* **2003**, *125*, 2641–51. (h) Stoebenau, E. J., III; Jordan, R. F. *J. Am. Chem. Soc.* **2003**, *125*, 3222–3. (i) Stoebenau, E. J., III; Jordan, R. F. *J. Am. Chem. Soc.* **2004**, *126*, 11170–1. (j) Stoebenau, E. J., III; Jordan, R. F. *J. Am. Chem. Soc.* **2006**, *128*, 8638–50. (k) Stoebenau, E. J., III; Jordan, R. F. *J. Am. Chem. Soc.* **2006**, *128*, 8162–75. (l) Casey, C. P.; Fisher, J. J. *Inorg. Chim. Acta* **1998**, *270*, 5–7. (m) Casey, C. P.; Fagan, M. A.; Hallenbeck, S. L. *Organometallics* **1998**, *17*, 287–9. (n) Crowther, D. J.; Swenson, D. C.; Jordan, R. F. *J. Am. Chem. Soc.* **1995**, *117*, 10403–4. (o) Galakhov, M. V.; Heinz, G.; Royo, P. *Chem. Commun.* **1998**, 17–8.
- (61) (a) Bosque, R.; Clot, E.; Fantacci, S.; Maseras, F.; Eisenstein, O.; Perutz, R. N.; Renkema, K. B.; Caulton, K. G. *J. Am. Chem. Soc.* **1998**, *120*, 12634–640. (b) Reinhold, M.; McGrady, J. E.; Perutz, R. N. *J. Am. Chem. Soc.* **2004**, *126*, 5268–76. (c) Clot, E.; Oelckers, B.; Klahn, A. H.; Eisenstein, O.; Perutz, R. N. *Dalton Trans.* **2003**, 4065–74.

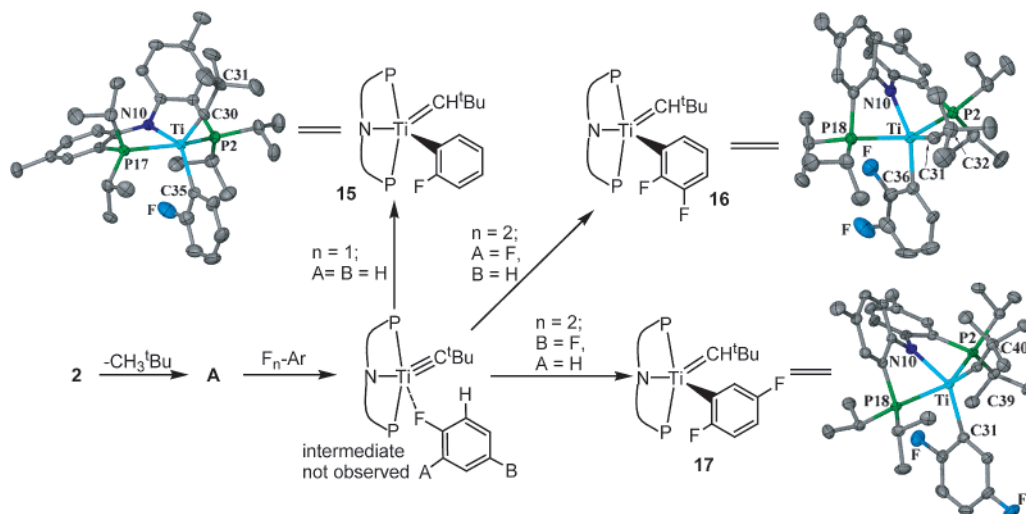
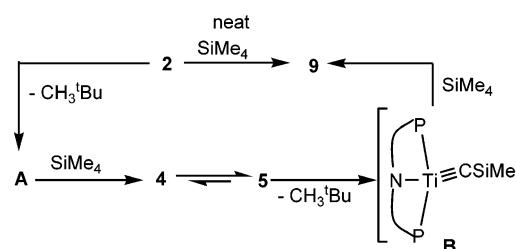


**Figure 9.** Synthesis of complexes **15**–**17** from precursor **2**. The molecular structures of each product are displayed with thermal ellipsoids at the 50% probability level. Solvent, disordered aryls, and H-atoms have been excluded for clarity. Selected metrical parameters (distances in angstroms, angles in degrees): For **15**, Ti–N10, 2.038(2); Ti–P2, 2.563(1); Ti–P17, 2.6175(9); Ti–C30, 1.865(3); Ti–C35, 2.138(6); Ti–C30–C31, 166.7(2); P2–Ti1–P17, 150.28(3). For **16**, Ti–N10, 2.040(4); Ti–P2, 2.6305(7); Ti–P18, 2.5692(8); Ti–C31, 1.866(7); Ti–C36, 2.173(7); Ti–C31–C32, 166.5(4); P2–Ti1–P18, 150.47(8). For **17**, Ti–N10, 2.060(2); Ti–P2, 2.5865(5); Ti–P18, 2.5589(5); Ti–C31, 2.210(6); Ti–C39, 1.864(6); Ti–C39–C40, 163.1(2); P2–Ti1–P18, 147.15(7).

cases. For all reactions, C–H bond activation of the arene typically occurs at 25 °C over 24 h. With the exception of toluene, *m*-xylene, and 1,3-difluorobenzene, activation of the arene C–H bond takes place exclusively ortho with respect to the F group. Given our proposed reaction profile (Figure 2), this result implies that coordination of such a group to **A** likely takes place prior to the C–H activation step. It is reasonable to speculate that binding of the arene substrate places the aryl C–H group proximal to the Ti≡C bond, to form the hypothetical intermediate “(PNP)Ti≡C<sup>t</sup>Bu(Ar<sup>t</sup>H)” displayed in Figure 9 (Ar<sup>t</sup>H = fluoroarene). This might explain why the aryl C–H bond proximal to the substituent is more amenable to activation.<sup>61</sup> However, given our mechanistic C–H activation study involving benzene, a species such as (PNP)Ti≡C<sup>t</sup>Bu(Ar<sup>t</sup>H) might be a side intermediate that does not lie directly on the C–H activation pathway, but rather rearranges to a  $\pi$ - and/or  $\sigma$ -complex. We are currently examining the basis for regioselectivity in compounds **15**–**17** by addressing the role of the fluoride in the C–H activation process since incipient negative charge at the *ortho*-carbon might be playing a crucial role in these types of reactions.

Our DFT studies suggest a dative fluorobenzene adduct, (PNP)Ti≡C<sup>t</sup>Bu(FC<sub>6</sub>H<sub>5</sub>), as a viable intermediate along the C–H bond activation step. Binding of FC<sub>6</sub>H<sub>5</sub> to **A** slightly perturbs the metrical parameters when compared to the computed structure of **A** (Figure 8). The long Ti–F distance of 2.269 Å and the F–C<sub>6</sub>H<sub>5</sub> distance of 1.398 Å are indicative of a weak interaction: in free fluorobenzene, the F–C<sub>6</sub>H<sub>5</sub> distance is ~1.36 Å.<sup>62</sup> In addition, the Ti–F distance observed in (PNP)Ti≡C<sup>t</sup>Bu(FC<sub>6</sub>H<sub>5</sub>) is much longer when compared to the only structural example of a Ti(IV)–FC<sub>6</sub>H<sub>5</sub> adduct (2.113(7) Å) for the cationic titanium imide salt [(nacnac)Ti=NAr(FC<sub>6</sub>H<sub>5</sub>)]-[B(C<sub>6</sub>F<sub>5</sub>)<sub>4</sub>]<sup>−</sup> (nacnac<sup>−</sup> = [ArNC(<sup>t</sup>Bu)]<sub>2</sub>CH, Ar = 2,6-*i*-Pr<sub>2</sub>C<sub>6</sub>H<sub>3</sub>).<sup>62</sup> Although the gas-phase electronic energy of (PNP)Ti≡C<sup>t</sup>Bu(FC<sub>6</sub>H<sub>5</sub>) is downhill by 9.78 kcal/mol, the free energy is uphill

#### Scheme 4



by 7.27 kcal/mol, due to the entropy and solvation penalties. This result implies that an adduct such as (PNP)Ti≡C<sup>t</sup>Bu(FC<sub>6</sub>H<sub>5</sub>) might be in a pre-equilibrium with intermediate **A**, and might explain why regioselectivity in the activation of the aryl C–H bond is not always observed.

Although NMR spectroscopic data for all cases were consistent with the proposed connectivity, we collected single-crystal X-ray diffraction data of compounds **15**–**17** to further confirm that activation of one aryl C–H bond is generally ortho to the F substituent. Although the molecular structures of **15** and **16** suffered from co-crystallization of the two aryl isomers (disorder from F pointing in and out of the C=Ti–C<sub>ipso</sub> groove), all structures are consistent with the proposed connectivity and clearly depict a short Ti=C bond and an obtuse Ti=C–C angle (Figure 9). In each molecular structure, the interaction between the Ti and the ortho group of the arene is negligible (Ti–F (**15**–**17**) > ~3.04 Å). Other pertinent features for the molecular structures of **15**–**17** are given in Figure 9.

#### 2.4. Intermolecular C–H Activation of Aliphatic Groups.

Complex **2** remains the most reactive alkylidene–alkyl species from our series and readily undergoes  $\alpha$ -H abstraction (CH<sub>3</sub><sup>t</sup>Bu is observed spectroscopically) in the presence of alkanes such as cyclohexane-*d*<sub>12</sub>, hexane-*d*<sub>14</sub>, and pentane-*d*<sub>12</sub> at 25 °C over 24 h. Unfortunately, reaction of **2** with these solvents is not clean, hampering characterization of the products. Despite these characterization problems, the most concrete evidence for an aliphatic C–H group stems from the clean transformation of **2** in neat SiMe<sub>4</sub> (90 °C, 12 h) to provide

(62) Basuli, F.; Aneetha, H.; Huffman, J. C.; Mindiola, D. J. *J. Am. Chem. Soc.* **2005**, *127*, 17992–3.

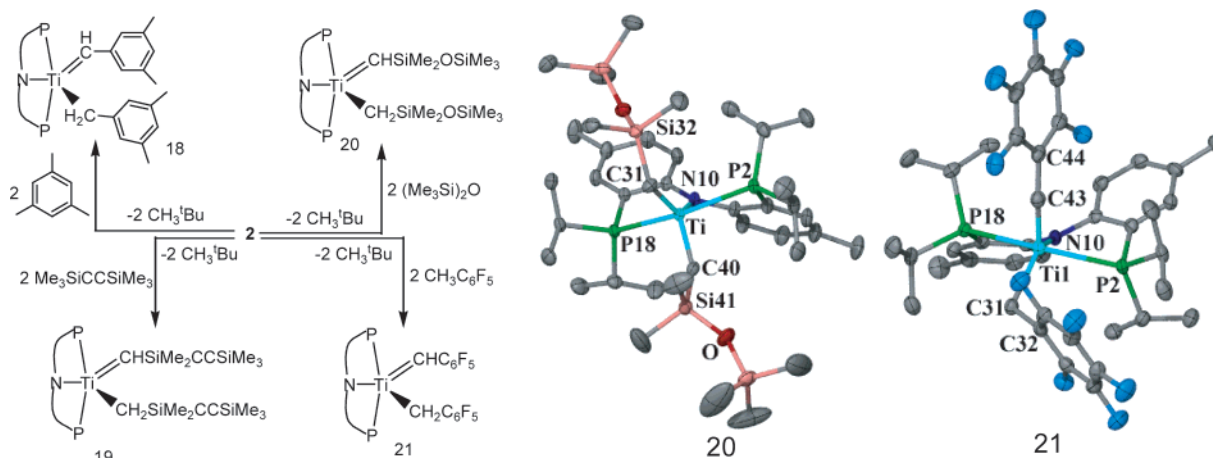
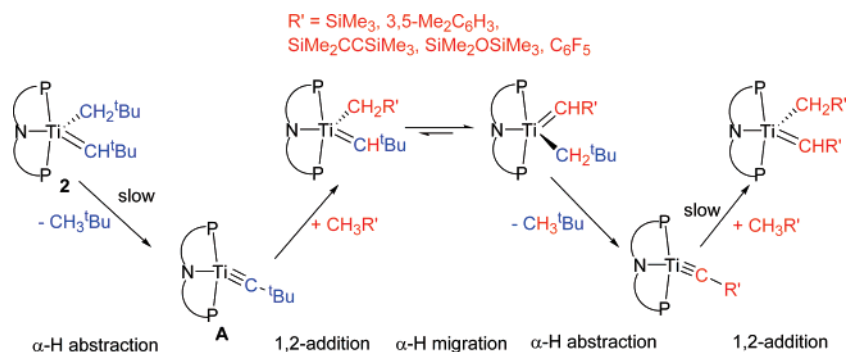


**Figure 10.** Multiple C–H activation reactions to prepare complexes **18–21**. The molecular structures of **20** and **21** are displayed, depicting thermal ellipsoids at the 50% probability level, with H-atoms excluded for clarity. Selected metrical parameters (distances in angstroms, angles in degrees): For **20**, Ti–N10, 2.072(1); Ti–P2, 2.594(4); Ti–P18, 2.6129(5); Ti–C40, 1.883(3); Ti–C31, 2.112(4); Ti–C31–Si32, 129.94(8); Ti–C40–Si41, 143.07(8); P2–Ti1–P18, 149.30(4). For **21**, Ti–N10, 2.015(9); Ti–P2, 2.6098(8); Ti–P18, 2.6181(8); Ti–C43, 1.891(3); Ti–C31, 2.191(3); Ti–C43–C44, 156.9(2); Ti–C31–C32, 115.4(7); P2–Ti1–P18, 153.02(3).

### Scheme 5



**9** (Scheme 4). The latter process indicates that  $\alpha$ -hydrogen abstraction,  $\alpha$ -hydrogen migration, and 1,2-CH bond addition processes are all playing a role along the reaction profile (Scheme 5). We propose that formation of **9** proceeds first via the rate-determining step,  $\alpha$ -hydrogen abstraction to generate intermediate **A**, which subsequently undergoes 1,2-CH bond addition of tetramethylsilane across the  $\text{Ti}=\text{C}^t\text{Bu}$  linkage to furnish the non-degenerate alkylidene–alkyl complex **4**. As noted previously with non-degenerate titanium alkylidene–alkyls, complex **4** is amenable to  $\alpha$ -hydrogen migration, thus equilibrating to **5**. By virtue of a second  $\alpha$ -hydrogen abstraction, intermediate **5** generates a second equivalent of  $\text{CH}_3^t\text{Bu}$  and the (trimethylsilyl)methylidyne intermediate  $(\text{PNP})\text{Ti}=\text{C}^t\text{SiMe}_3$  (**B**), and the latter undergoes activation of another C–H bond of tetramethylsilane (which is present in large excess) to ultimately produce **9** (Schemes 4 and 5). In fact, independent experiments confirm that the **4/5** mixture (isolated from **2** and  $\text{LiCH}_2\text{SiMe}_3$  in  $\text{C}_6\text{H}_{12}$ , vide supra) cleanly reacts with tetramethylsilane to afford **9**, therefore suggesting that these are viable intermediates along the **2**  $\rightarrow$  **9** transformation. Formation of **9** from **2** involves an unprecedented activation of three  $sp^3$  C–H bonds of solvent under mild conditions by a transition metal complex,<sup>63</sup> thereby insinuating that the  $\text{Ti}=\text{C}^t\text{SiMe}_3$  functionality in **B** is far more within reach thermodynamically than the prototypical  $\text{Ti}=\text{C}^t\text{Bu}$  ligand in **A**.

Moreover, the net activation of three  $sp^3$  C–H bonds of solvent is not limited to  $\text{SiMe}_4$  alone, inasmuch as hydrocarbons can be similarly cleaved under mild conditions. For example, **2** can also break three benzylic C–H bonds of 1,3,5-trimethylbenzene to yield  $(\text{PNP})\text{Ti}=\text{CH}\{3,5\text{-Me}_2\text{C}_6\text{H}_3\}(\text{CH}_2\{3,5\text{-Me}_2\text{C}_6\text{H}_3\})$  (**18**) quantitatively (Figure 10; see Supporting Information for spectroscopic details). Monitoring the reaction by  $^{31}\text{P}\{^1\text{H}\}$  NMR identifies two intermediates, likely the tautomers  $(\text{PNP})\text{Ti}=\text{CH}^t\text{Bu}(\text{CH}_2\{3,5\text{-Me}_2\text{C}_6\text{H}_3\})/(\text{PNP})\text{Ti}=\text{CH}\{3,5\text{-Me}_2\text{C}_6\text{H}_3\}(\text{CH}_2^t\text{Bu})$ , which form and decay over 48 h at 45 °C to ultimately produce **18** (Figure 10). Other reagents, such as  $\text{Me}_3\text{SiC}\equiv\text{CSiMe}_3$ ,  $(\text{Me}_3\text{Si})_2\text{O}$ , and  $\text{MeC}_6\text{F}_5$ , also react cleanly with **2** to generate a sole product resulting from triple C–H activation of the methyl groups of the substrate, to produce the compounds  $(\text{PNP})\text{Ti}=\text{CHSiMe}_2\text{CCSiMe}_3(\text{CH}_2\text{SiMe}_2\text{CCSiMe}_3)$  (**19**),  $(\text{PNP})\text{Ti}=\text{CHSiMe}_2\text{OSiMe}_3(\text{CH}_2\text{SiMe}_2\text{OSiMe}_3)$  (**20**), and  $(\text{PNP})\text{Ti}=\text{CHC}_6\text{F}_5(\text{CH}_2\text{C}_6\text{F}_5)$  (**21**) (Figure 10). We believe that formation of **19–21** also proceeds by a combination of two  $\alpha$ -hydrogen abstraction steps, one  $\alpha$ -hydrogen migration, and two 1,2-CH bond additions across two different transient titanium alkylidyne intermediates, the first of which entails **A** (Scheme 5). Complexes **18–21** have also been fully characterized by  $^1\text{H}$ ,  $^{13}\text{C}$ , and  $^{31}\text{P}$  NMR spectra. Most remarkably, the molecular structures of **20** and **21** portray unique examples of transition metal complexes containing a trimethylsilyl ether or perfluoroaryl-substituted alkylidene moiety ( $\text{Ti}=\text{C}$ , 1.883(3) Å, **20**;  $\text{Ti}=\text{C}$ , 1.891(3) Å, **21**, Figure 10).

(63) (a) Lee, J.-H.; Pink, M.; Caulton, K. G. *Organometallics* **2006**, *25*, 802–4. (b) Ozerov, O. V.; Pink, M.; Watson, L. A.; Caulton, K. G. *J. Am. Chem. Soc.* **2004**, *126*, 2105–13.

### 3. Conclusions

In this work, we have demonstrated that titanium alkylidene–alkyl complexes can undergo  $\alpha$ -hydrogen abstraction reactions smoothly to generate transient titanium alkylidyne intermediates, which display a remarkably versatile reactivity toward unactivated C–H bonds in a number of common solvents. While intramolecular C–H activation of an aryl moiety by a tungsten neopentylidyne has been documented,<sup>64</sup> our work clearly shows the first example of intermolecular C–H bond-breaking processes promoted by  $Ti\equiv C$  linkages.<sup>64</sup> We have utilized an integrated approach combining experimental and theoretical tools at our disposal to examine the mechanistic details of these novel chemical transformations. The  $\alpha$ -hydrogen abstraction step leading to the reactive intermediate that contains an unprecedented  $Ti\equiv C$  linkage is rate-determining in all cases that we considered. The titanium alkylidyne complex undergoes facile 1,2-CH bond addition of hydrocarbons or close derivatives thereof across the polarized  $Ti\equiv C$  bond to yield new alkylidene–alkyl products. When benzene is used as a reactant, the thermodynamic product can slowly equilibrate back, at temperatures above 95 °C, to the alkylidyne intermediate, thereby creating an independent route to the alkylidyne functionality in benzene from the post-rate-determining step. The notion that the titanium alkylidyne functionality can be formed from a starting material such as **2** or a thermodynamic product such as **3** offers an excellent opportunity to not only study C–H activation reactions in neat solvent using **2** as the precursor, but also conduct stoichiometric reactions in camouflaging solvents such as benzene by employing **3** as the precursor. Our kinetic studies, from both theoretical and experimental standpoints, suggest that a  $\sigma$ -complex (**14**) is formed along the C–H bond activation step, which takes place in a heterolytic fashion to afford a highly charge-polarized transition state. C–H bond activation and rupture are promoted by the LUMO of **A** in concert with the HOMO orbital, the latter serving as a potent nucleophile in the 1,2-CH addition process. We established that the reactivity of the alkylidyne functionality follows a decreasing trend in the order  $Ti\equiv C^tBu \gg Ti\equiv CSiMe_3 \geq Ti\equiv CPh$ . In most cases, aryl C–H activation of substituted arenes is preferred over aliphatic C–H bonds since the group of the aryl motif heavily directs orthometalation via coordination to the low-coordinate and transient intermediate  $(PNP)Ti\equiv C^tBu$ . In general, it appears that intermolecular C–H activation reactions are

governed kinetically, since activation of the least hindered C–H group is typically observed. In some cases, however, the combination of two  $\alpha$ -hydrogen abstractions, an  $\alpha$ -hydrogen migration, and two 1,2-CH bond additions can result in the net cleavage of five C–H bonds, three of which derive from solvent molecules. This series of well-understood reactions that include multiple C–H bond cleavages, two of which were intermolecular while three were intramolecular, has allowed us to incorporate novel substituted alkylidene moieties onto the titanium center. Therefore, this new process can be best defined as an alkylidene–alkyl metathetical reaction with hydrocarbons, whereby alkylidene and alkyl moieties exchange with two equivalents of hydrocarbon species. The search for systems properly tuned for the stabilization of a terminal titanium alkylidyne is an ongoing project in our laboratory since this parameter will allow us to selectively harness the intrinsic power stored in the  $Ti\equiv C$  linkage. Although the work discussed in this paper encompasses stoichiometric reactions, a mechanistic understanding of the intermolecular binding and activation of C–H bonds represents an important step toward the rational and selective functionalization of inert substrates with low binding affinities. This parameter could, in principle, aid future efforts for the systematic design of more efficient catalysts involved in processes such as hydrocracking and alkane metathesis.

**Acknowledgment.** We thank Indiana University–Bloomington, the Dreyfus Foundation, the Sloan Foundation, NSF (CHE-0348941, PECASE Award to D.J.M.; CHE-0645381 to M.-H.B.), and NIH (HG003894 to M.-H.B.) for financial support of this research. M.-H.B. is a Cottrell Scholar of the Research Corporation. B.C.B. acknowledges the Department of Education and the Lubrizol Foundation for Fellowships. The authors thank Prof. P. T. Wolczanski for advice and insightful suggestions, and all of the reviewers for providing invaluable feedback on this work.

**Supporting Information Available:** Complete kinetic data (conversions of **2** to **3** and **3** to **3-d<sub>6</sub>**, KIEs, EIEs), synthetic and spectroscopic NMR data for all compounds, and computational details (**2**, **3**, relevant intermediates along the **2**  $\rightarrow$  **3** coordinate, other viable pathways and intermediates, and  $(PNP)Ti\equiv C^tBu$  ( $\sigma$ - $FC_6H_5$ )) (PDF). X-ray crystallographic data for compounds **11**, **12**, **15–17**, **20**, and **21** (CIF). This material is available free of charge via the Internet at <http://pubs.acs.org>.

(64) Couturier, J. L.; Paillet, C.; Leconte, M.; Basset, J. M.; Weiss, K. *Angew. Chem.* **1992**, *104*, 622–4.

JA070989Q